Cerebral Cortex September 2009;19:2196–2207
doi:10.1093/cercor/bhp009
Advance Access publication February 20, 2009

Selective Depletion of Molecularly Defined Cortical Interneurons in Human Holoprosencephaly with Severe Striatal Hypoplasia

Sofia Fertuzinhos[1,2], Željka Krsnik[1], Yuka Imamura Kawasawa[1], Mladen-Roko Rašin[1], Kenneth Y. Kwan[1], Jie-Guang Chen[1], Miloš Judaš[3], Masaharu Hayashi[4] and Nenad Šestan[1]

[1]Department of Neurobiology and Kavli Institute for Neuroscience, Yale University School of Medicine, New Haven, CT 06510, USA, [2]Doctoral Program in Experimental Biology and Biomedicine, University of Coimbra, 3004-517 Coimbra, Portugal, [3]Croatian Institute for Brain Research, University of Zagreb School of Medicine, 10 000 Zagreb, Croatia and [4]Department of Clinical Neuropathology, Tokyo Metropolitan Institute for Neuroscience, Tokyo 183-8526, Japan

Cortical excitatory glutamatergic projection neurons and inhibitory GABAergic interneurons follow substantially different developmental programs. In rodents, projection neurons originate from progenitors within the dorsal forebrain, whereas interneurons arise from progenitors in the ventral forebrain. In contrast, it has been proposed that in humans, the majority of cortical interneurons arise from progenitors within the dorsal forebrain, suggesting that their origin and migration is complex and evolutionarily divergent. However, whether molecularly defined human cortical interneuron subtypes originate from distinct progenitors, including those in the ventral forebrain, remains unknown. Furthermore, abnormalities in cortical interneurons have been linked to human disorders, yet no distinct cell population selective loss has been reported. Here we show that cortical interneurons expressing nitric oxide synthase 1, neuropeptide Y, and somatostatin, are either absent or substantially reduced in fetal and infant cases of human holoprosencephaly (HPE) with severe ventral forebrain hypoplasia. Notably, another interneuron subtype normally abundant from the early fetal period, marked by calretinin expression, and different subtypes of projection neuron were present in the cortex of control and HPE brains. These findings have important implications for the understanding of neuronal pathogenesis underlying the clinical manifestations associated with HPE and the developmental origins of human cortical interneuron diversity.

Keywords: basal ganglia, brain evolution, cerebral cortex, developmental disorder, interneuronopathy, nitric oxide

Introduction

Holoprosencephaly (HPE), the most common human congenital brain malformation, is often associated with motor deficits, seizures, and mental retardation (Probst 1979; Golden 1999; Muenke and Beachy 2000; Monuki 2007; Fernandes and Hébert 2008). HPE is characterized by inadequate separation of the 2 cerebral hemispheres due to abnormal embryonic development of the forebrain midline. Typically, HPE cases are classified, in order of increasing severity, as lobar, semilobar, or alobar, according to the degree of dorsal midline fusion of the cerebral hemispheres (DeMyer 1977; Probst 1979; Barkovich and Quint 1993; Takahashi et al. 2004). However, the majority of HPE brains also exhibit a spectrum of defects in the development and midline separation of ventral forebrain structures, including the striatum, ranging from moderately affected to severely hypoplastic (Yakovlev 1959; Probst 1979; Barkovich and Quint 1993; Golden 1999). Studies in experimental animals suggest that defects in ventral midline progenitor cells lead to specific alterations in the development of ventral forebrain structures, including the ganglionic eminences and striatum, often without severely affecting the specification of cortical neuronal progenitors and excitatory glutamatergic projection neurons in the dorsal forebrain (Cheng et al. 2006; Rash and Grove 2007; Fernandes and Hébert 2008). However, whether defects of human ventral midline development, in cases of HPE or other diseases, affect neocortical and hippocampal inhibitory GABAergic interneurons has not been examined.

Previous postmortem studies of human HPE brains were limited to the analysis of neuronal morphology and expression of a few pan-neuronal markers (Yakovlev 1959; Probst 1979; Mizuguchi and Morimatsu 1989; Golden 1999; Arii et al. 2000; Judas et al. 2003; Hayashi et al. 2004), leaving open the possibility that molecularly and functionally distinct cortical neuronal cell types are selectively affected or absent in human HPE. Cortical interneurons comprise a great variety of morphologically and molecularly identifiable subtypes (Kawaguchi and Kondo 2002; Wonders and Anderson 2006; Petilla Interneuron Nomenclature Group 2008). Most of these subtypes are common to all mammals; however, some subtypes exhibit prominent evolutionary differences in their number, molecular profile, morphology, and functional organization (Jones 1993; Gabbott and Bacon 1996; DeFelipe et al. 2006; Meyer 2007).

Recent experimental evidence indicates that in mice and ferrets, a large majority of cortical interneurons share a common origin with striatal neurons, arising from progenitors within the ventral forebrain and migrating dorsally into the cortex (Anderson et al. 1997; Métin et al. 2006). In humans, however, it has been proposed, without reference to specific subpopulations, that the majority of cortical interneurons arise from dorsal, instead of ventral, forebrain progenitors (Letinic et al. 2002). Due to variations in human HPE cases in their ventral forebrain phenotypes, we hypothesize that in HPE cases with severe hypoplasia of the striatum, but not those with little or no defects in ventral forebrain, specific subpopulations of cortical interneurons would either be greatly reduced in number or absent. To test our hypothesis, we undertook detailed characterization of the various distinct cortical neuronal cell types in fetal and infant human HPE cases with severe striatum hypoplasia and those with moderately to well-differentiated striatum, as well as in age-matched normal control brains. Our results show that a distinct subpopulation of interneurons coexpressing nitric oxide synthase 1 (*NOS1*), neuropeptide Y (*NPY*), and somatostatin (*SST*) is consistently absent or substantially reduced from the neocortex and hippocampus of HPE cases with severe ventral forebrain midline and striatal hypoplasia. In contrast, calretinin (CALB2)-positive neurons, the other major subtype of cortical interneurons normally abundant from the early fetal period, as well as multiple subtypes of excitatory projection neurons are clearly

present in the neocortex and hippocampus of all examined control and HPE brains. The correlation between the selective absence of molecularly defined cortical interneurons and the severity of disruption of the ventral forebrain midline in some cases of HPE suggests that human cortical interneuron subtypes are derived from distinct progenitors and that molecularly defined subpopulations may originate in the ventral forebrain and migrate dorsally into the cortex.

Materials and Methods

Brain Specimens

This study was carried out using postmortem human brain specimens (Supplementary Tables 1 and 2) collected according to guidelines on the research use of human brain tissue from the New York State–licensed Human Fetal Tissue Repository at the Albert Einstein College of Medicine (AECOM); the Department of clinical neuropathology of the Tokyo Metropolitan Institute for Neuroscience (TMIN); and the Croatian Institute for Brain Research (CIBR) at the University of Zagreb School of Medicine. This study was approved by the Human Investigation Committees at the Yale University School of Medicine and the 3 above-mentioned institutions. For each tissue donation, appropriate maternal written informed consent and approval were obtained. We recorded all available nonidentifying information, including maternal medical history, age, and ethnicity and fetus/infant gender, weight, cause of death, medications, Apgar score, and relevant medical conditions. The fetal age was determined by the date of last menstruation, ultrasonographic scanning, crown-rump length, and/or foot length.

Fourteen brains with no signs of malformations or brain lesions were used as controls (Ctrl-1 to -14; Supplementary Table 1). Specific agonal conditions, including coma, hypoxia, pyrexia, seizures, dehydration, hypoglycemia, multiple organ failure, head injury, and ingestion of neurotoxic substances at time of death, were grounds for exclusion. All HPE cases had brain and midfacial abnormalities typical of HPE and were organized according to: 1) age and 2) state of ventral forebrain midline and striatum development from moderately and well-differentiated (group A) to hypoplastic (group B; Supplementary Table 2). In group B cases (HPE-B), the striatum was severely hypolastic and fused to the thalamus, forming single centroventrally positioned rudimentary striatothalamic eminence (Fig. 1*a*). The average postmortem delay prior to fixation was 1.9 ± 0.9 h for control brains and 2.5 ± 0.7 h for HPE brains ($P > 0.05$). The average fetal and postnatal age were, respectively, 23.5 ± 1.7 weeks of gestations (wg) and 6.3 ± 2.8 months for control brains and 25.7 ± 2.5 wg and 5.2 ± 2.0 months for HPE brains ($P > 0.05$).

Tissue Processing

The HPE and age-matched control specimens, obtained from the Human Fetal Tissue Repository at the AECOM, were collected in cold phosphate buffered saline (PBS), separated from surrounding tissue, and immediately dissected into approximately 1 cm thick slabs and fixed in 4% (w/v) paraformadehyde (PFA)/PBS for 48 h at 4 °C. For specimens obtained from AECOM, we examined the whole brain in all controls and the neocortex and hippocampus in all HPE cases. In HPE-2A, -3B, and -4B specimens, the striatum (HPE-2A) or the hypoplastic striatothalamic eminence (HPE-3B and -4B) as well as the thalamus, brain stem, and cerebellum were obtained and examined. In HPE-1A, the ventral forebrain (ganglionic eminences and basal ganglia), thalamus, brain stem, and cerebellum were not available for study. Following fixation, tissue slabs were cryoprotected in graded sucrose solutions [10%, 20%, and 30% (w/v) in PBS] at 4 °C, embedded in Tissue-Tek O.C.T. (Sakura Finetek USA, Inc., Torrance, CA), frozen at –40 °C in 2-methylbutane (J.T. Baker, Inc., Philipsburg, NJ), and stored at –80 °C. Tissue sections (30 and 60 μm thick) were prepared using a Leica CM3050S cryostat and mounted onto Superfrost/Plus slides (Fisher Scientific Co., Pittsburgh, PA) or stored as free-floating sections in PBS at 4 °C.

The HPE and control specimens (Supplementary Tables 1 and 2) obtained from the TMIN were fixed by immersion in formalin for 10–14 days, dissected into slabs and paraffin embedded. For all control and HPE cases, tissue sections of the frontal and temporal neocortex, hippocampus, striatum/striatothalamic eminence, and pons were analyzed.

The HPE and control specimens (Supplementary Tables 1 and 2) obtained from the CIBR were fixed by immersion in 4% PFA for at least 3 days. The HPE-9 brain was dissected into 1–2 cm thick slabs, cryoprotected, and frozen. For Ctrl-12 and HPE-7A brains, one tissue slab containing the ventral forebrain and frontal neocortex was processed for NADPH-diaphorase (NADPH-d) histoenzymatic staining. The remaining tissue slabs were embedded in paraffin.

Fourteen main control brains are listed by their ages in wg (fetal) or months (infants) (Supplementary Table 1). In addition, over 50 control brains not included in this present study, ranging in age from 12 wg to adult, were analyzed for NADPH-d staining, NOS1 immunohistochemistry, and expression of some of the cell type-specific markers listed in Supplementary Table 3, as part of previously published studies (Sajin et al. 1992; Sestan and Kostovic 1994; Judas et al. 1999). Data from these previous studies were used for making normative comparisons.

Immunohistochemistry

For immunohistochemical staining, slide-mounted (30 or 60 μm), or free-floating (60 μm) tissue sections were first washed in PBS and quenched with 1% hydrogen peroxide, prepared in PBS, to block endogenous peroxidase activity. Next, the sections were washed in PBS and incubated in blocking solution (BS) containing 5% (v/v) normal donkey serum (Jackson ImmunoResearch Laboratories, West Grove, PA), 1% (w/v) bovine serum albumin, 0.1% (w/v) glycine, 0.1% (w/v) L-lysine, and 0.4% (v/v) Triton X-100 in PBS for 1 h at room temperature (RT). Sections were then incubated overnight at 4 °C in primary antibodies (Supplementary Table 3) diluted in BS. For immunofluorescent staining, tissue sections were incubated with appropriate donkey secondary antibodies conjugated to different fluorophores (Jackson ImmunoResearch Labs), mounted and imaged using a Zeiss LSM 510 laser-scanning microscope. For 3,3′-diaminobenzidine (DAB) immunohistochemistry, sections were incubated in the appropriate donkey biotinylated secondary antibodies (Jackson ImmunoResearch Labs) diluted 1:250 in PBS for 1.5–2 h at RT. Following washing in PBS, sections were incubated in avidin–biotin–peroxidase complex (Vectastain ABC Elite kit; Vector Laboratories, Burlingame, CA) for 1 h at RT. Sections were washed in PBS (3 × 15 min) and incubated for 5 min in 20 mL of PBS containing 0.05% (w/v) DAB, 0.04% (w/v) ammonium chloride, 0.5–1 mg glucose oxidase type VII, and 80 μl of 0.05 M nickel ammonium sulfate in 0.2 M acetate buffer (pH 6.0). The peroxidase reaction was started by adding 400 μl of 10% (w/v) D-glucose/PBS and stopped 5–10 min later by washing in PBS. Finally, sections were dehydrated and mounted in Permount (Fisher Scientific Co.). The same protocol was followed in 10 μm paraffin embedded tissue slices after deparaffinization in xylene and rehydration in graded ethanol baths. All immunostainings were performed in at least 2 different control brains. Whenever possible, multiple antibodies against a specific cellular marker were used (Supplementary Table 3).

NADPH-d Histochemistry

NADPH-d histoenzymatic staining was performed as previously described (Sajin et al. 1992; Judas et al. 1999). Briefly, free-floating or slide-mounted tissue sections of control and HPE brains were incubated in medium containing 1 mM beta-NADPH (Sigma, St. Louis, MO), 0.8 mM nitro blue tetrazolium, and 0.3% Triton X-100 in 0.1 M PBS (pH 8.0) at 37 °C for 3–10 h. After incubation, sections were washed 3× in PBS and mounted on glass slides. Intensely reactive interneurons were easily identified by the high content of dark blue formazan precipitates. Intense staining of many blood vessels for NADPH-d (due to endothelial nitric oxide synthase 3) and a widespread faint staining of projection neurons served as internal positive controls. Intensely NADPH-d-reactive or NOS1-positive cortical interneurons were found in all fetal (starting at 15 wg) and postnatal control brains (Supplementary Table 1), as well as in over 50 control brains analyzed in previously published studies (Sajin et al. 1992; Sestan and Kostovic 1994; Judas et al. 1999).

RNA in situ Hybridization

For in situ hybridization, free-floating cryosections (60 μm) were postfixed with 4% PFA/PBS for 15 min, washed in PBS 3× 5 min, and hybridized overnight at 70 °C with 500 ng/mL of digoxigenin (DIG)-labeled cRNA probe corresponding to nucleotides 361-1506 of human *FEZF2* (NM_018008). The signal was detected with an alkaline phosphatase-conjugated anti-DIG antibody and NBT/BCIP chromogen (Roche Applied Science, Indianapolis, IN).

Quantifications and Statistical Analysis

Quantification of percentage of NADPH-d/NOS1- and CALB2-positive interneurons was performed in the neocortical and hippocampal cortical plate (CP) and subplate (SP) of all HPE and age-matched control brains, using StereoInvestigator software (MicrobrightField, Williston, VT). Neocortical tissue sections were immunostained for each interneuron marker and counterstained with Nissl. In each section, three locations were randomly selected for neuronal quantification. In each location, CP and SP were delineated and total cellular density was estimated in both by counting Nissl-stained cell bodies in randomly sampled optical dissectors (1225 μm^2 and 3–10 μm thick). Interneurons were counted in columns 536–2200 μm wide along the entire height of the CP and SP and throughout the total slice thickness (10 or 30 μm). Cellular density of each interneuron subtype was averaged across the 3 sampled locations and expressed in percentage. The distribution of cells immunolabeled for ASCL1 (also known as MASH1) or TITF1 (also known as NKX2.1), as well as the percentage of cell nuclei double immunolabeled for ASCL1 and Ki67 or TITF1 and Ki67, was estimated in the different fetal zones of the ventral and dorsal forebrain of midfetal Ctrl-1 (18 wg) and Ctrl-2 (20 wg) brains using 30 μm sections at ×40 amplification. The nonparametric Mann–Whitney *U* test was employed to assess possible significant differences ($P \leq 0.05$).

Results

Depletion of NOS1/NPY/SST-Positive Cortical Interneurons in Human HPE Brains with Severe Striatal Hypoplasia

To determine whether any major subtypes of cortical interneurons or projection neurons are affected in human fetal and infant HPE, we analyzed the expression of various neuronal cell type–specific markers using immunohistochemistry, histochemistry, and in situ hybridization (Supplementary Table 3). The analysis was performed in postmortem HPE brains with moderately to well-differentiated striatum (group HPE-A; $n = 3$), HPE brains with severe ventral forebrain midline and striatal hypoplasia (group HPE-B; $n = 8$), and age-matched midfetal to infant control brains ($n = 14$) with no signs of neuroanatomical abnormalities (Fig. 1*a*; Supplementary Tables 1 and 2). In HPE-B cases, the severely hypoplastic ventral forebrain, containing the rudimentary ganglionic eminences and striatum, was greatly reduced in size and intermingled with the thalamus, forming a small striatothalamic eminence along the ventral midline. This dramatic disruption of the ventral forebrain led us to hypothesize that cortical GABAergic interneurons, or specific subtypes thereof, could be

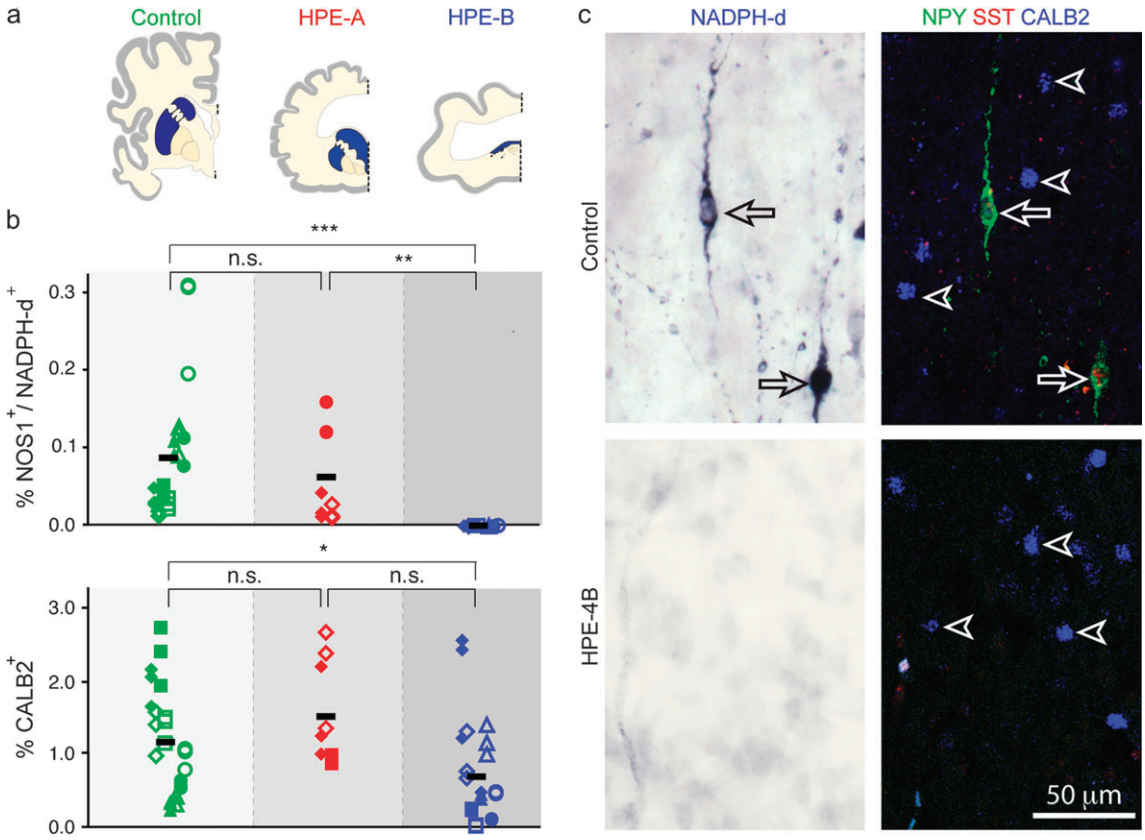

Figure 1. Selective absence of NOS1/NPY/SST-positive but not CALB2-positive cortical interneurons from fetal and early postnatal HPE brains with severe ventral forebrain (striatal) hypoplasia. (*a*) Schematic coronal forebrain sections with striatum (blue) in control and HPE-A brains and the rudimentary striatothalamic eminence (blue) in HPE-B brains. Midline is denoted by dashed line. (*b*) Quantification of NOS1/NADPH-d-positive and CALB2-positive neocortical interneurons as a percentage of total number of Nissl stained cells in controls (green; $n = 14$), group HPE-A (red; $n = 3$), and HPE-B (blue; $n = 8$) (n.s., not significant; $^*P \leq 0.05$; $^{**}P \leq 0.0001$; $^{***}P \leq 0.00001$). (*c*) Neocortex of HPE-4B (bottom) and age-matched control (top) stained for NADPH-d (left, blue) and triple immunofluorescence (right) for NPY (green), SST (red), and CALB2 (blue). Arrows depict neurons coexpressing NADPH-d, NPY, and SST. Arrowheads depict CALB2-immunolabeled neurons.

affected in group HPE-B brains. Normally, 2 major subtypes molecularly and functionally distinct of human cortical interneurons are clearly present from the early fetal period: CALB2- and NOS1/NPY/SST-expressing interneurons (Judas et al. 1999; Meyer 2007). At this developmental stage, we found that calbindin 1 (CALB1)-positive interneurons were scarcely present in the marginal zone (MZ) of the hippocampus and were almost completely absent from the neocortex (Supplementary Table 4; data not shown). Together with parvalbumin (PVALB)-expressing interneurons, they mainly appear in the neocortex later in development during late fetal period and early infancy (Judas et al. 1999; Ulfig 2002; Meyer 2007). During the midfetal period, we found numerous GABA- and CALB2-positive interneurons in the striatum, neocortex, and hippocampus of both group HPE-A and -B, as well as in age-matched control brains (Figs. 1*b,c* and 2*a,b*). In contrast, interneurons positive for NOS1/NPY/SST or NADPH-d, a histoenzymatic marker of all isoforms of NOS, were almost completely missing from the SP, CP, and MZ of the neocortex and hippocampus of all HPE-B cases and moderately reduced in HPE-A cases compared with age-matched control brains (Figs. 1*b,c*, 2*c–e*, and 3*b–d*).

To show that the midfetal absence of molecularly defined cortical interneurons is not due to delayed migration or differentiation, we analyzed HPE cases from the late fetal period and early infancy from both groups A and B (Supplementary Table 2). Consistent with results from our midfetal analysis, late fetal and early infant HPE-A and -B cases contained CALB2-positive interneurons comparable in number and morphological maturation to age-matched controls (Fig. 4*a*; Supplementary Table 4). Also consistent with the midfetal findings, NOS1/NPY/SST-positive interneurons were either absent or dramatically reduced from the neocortex and hippocampus of late fetal and infant HPE-B cases (Fig. 4*d3,4;e3,4;f3,4*).

Because a significant number of PVALB- and CALB1-positive interneurons are present in the human cortex around the time of birth (Judas et al. 1999; Ulfig 2002; Meyer 2007), we were also able to analyze the differentiation and distribution of these interneurons in late fetal and infant cases. PVALB-positive interneurons were observed in the neocortex and hippocampus of some late fetal and infant control and HPE-A brains (Fig. 4*bc1,2*; Supplementary Table 4). However, these interneurons were either absent or substantially reduced in the neocortex and hippocampus of HPE-B brains. In the same tissue sections of HPE-B brains, moderate immunostaining of pyramidal neurons was present in neocortical layer 5 (data not shown), indicating that the absence of PVALB-positive interneurons was not due to staining failure. However, a negligible number of PVALB-positive neurons was observed in the deep white matter of only 1 HPE case from group B (HPE-9B). The large soma size and the pattern of dendritic arborization of these white matter PVALB-positive neurons in HPE-9B were reminiscent of white matter interstitial neurons previously described in human infants (Judas et al. 1999; Ulfig 2002; Meyer 2007), the characteristics of which have not been well studied. Though PVALB-positive interneurons appear to be severely depleted from the cortex of late fetal and infant HPE-B cases, additional specimens of these stages are needed to substantiate this observation.

Previous studies have shown that CALB1 is substantially coexpressed by both PVALB- and NOS1/NPY/SST-positive interneurons and to a lesser extent by CALB2-positive interneurons (Kubota et al. 1994; Markram et al. 2004). We observed CALB1-positive cortical interneurons mainly in the layer 1, SP, and white matter of late fetal and infant control and HPE-A neocortical wall (Fig. 4*b*). Even though in apparently reduced numbers, CALB1-positive cortical interneurons were observed in the neocortical wall and hippocampus of late fetal

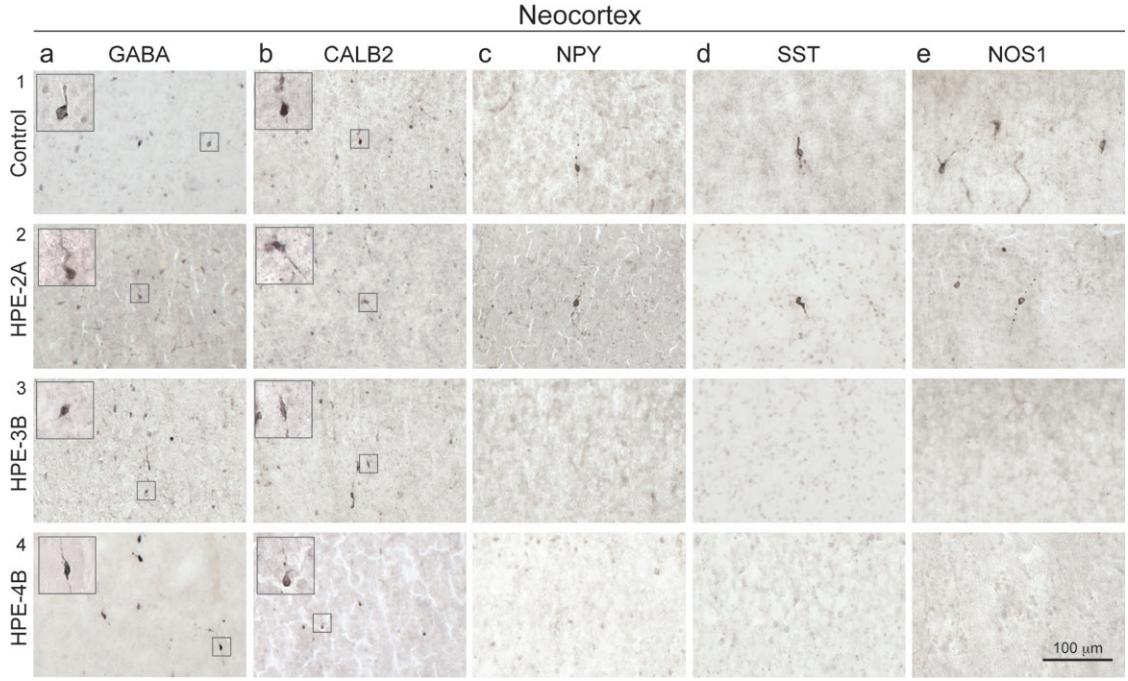

Figure 2. Representative images of immunohistochemical staining for different molecular markers of interneurons in midfetal control and HPE-2A, -3B, and -4B brains. (*a1–4, b1–4*) Numerous GABA- and CALB2-positive cortical interneurons are present at the border between the CP and SP of both control and all HPE brains. (*c3,4-e 3, 4*), NOS1-, NPY-, and SST-positive cortical interneurons are absent from the CP and SP of HPE-B brains.

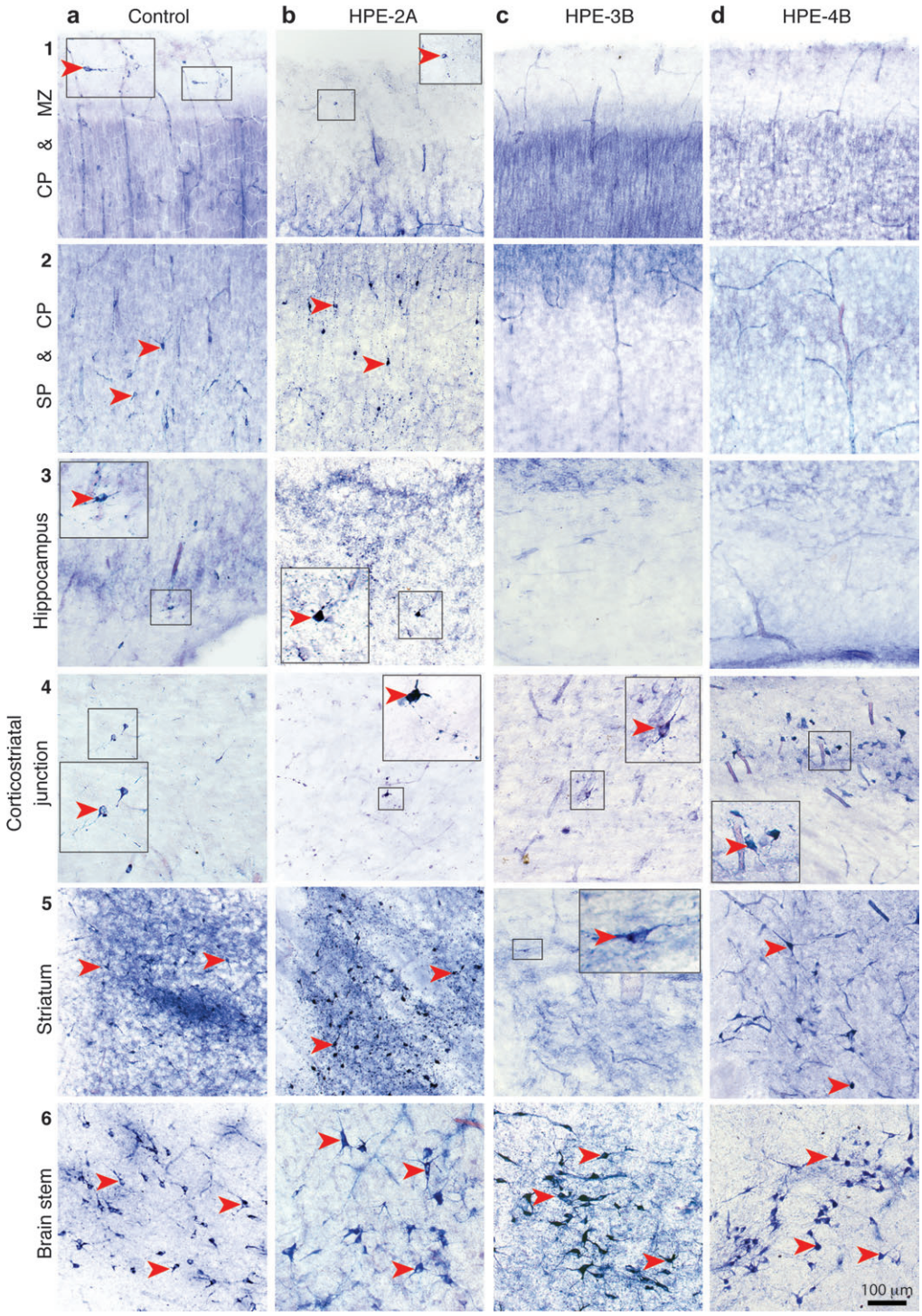

Figure 3. Histochemical staining for NADPH-d, a marker of NOS, in different regions of the forebrain and in the pedunculopontine nucleus of the brain stem in a control brain (20 wg) and HPE-2A, HPE-3B, and HPE-4B brains. (*a1–5, b1–5*) Large interneurons intensely reactive for NADPH-d (red arrowheads) were present in the MZ, CP, SP, and fetal white matter of the neocortical wall, hippocampus, and striatum of a 20 wg control fetal brain and HPE-2A. (*c1–4, d1–4*) HPE-3B and -4B brains contain no intensely reactive NADPH-d interneurons in the neocortical or hippocampal MZ, CP, or SP. (*c5, d5*) Only in HPE-4B could large intensely NADPH-d-positive interneurons be detected in nodular heterotopias in the fetal white matter, at the border of the neocortical wall and midline mass containing the rudimentary striatothalamic eminence. (*a6-d6*) NADPH-d-positive neurons were also present in the brain stem of all cases. Intense staining of blood vessels (due to endothelial NOS3) and a widespread faint staining of projection neurons (due to neuronal NOS1) for NADPH-d served as internal positive controls for all brains. Insets show enlarged views of the indicated area.

and infant HPE-B brains. These observations are consistent with our findings of dramatic depletion of NOS1/NPY/SST-positive but not CALB2-positive cortical interneurons, both of which can express *CALB1*. Taken together, these analyses show that cortical interneurons molecularly defined by the expression of NOS1, NPY, and SST are consistently either absent or substantially reduced in the cortex of fetal and infant group B HPE cases with severe ventral forebrain hypoplasia.

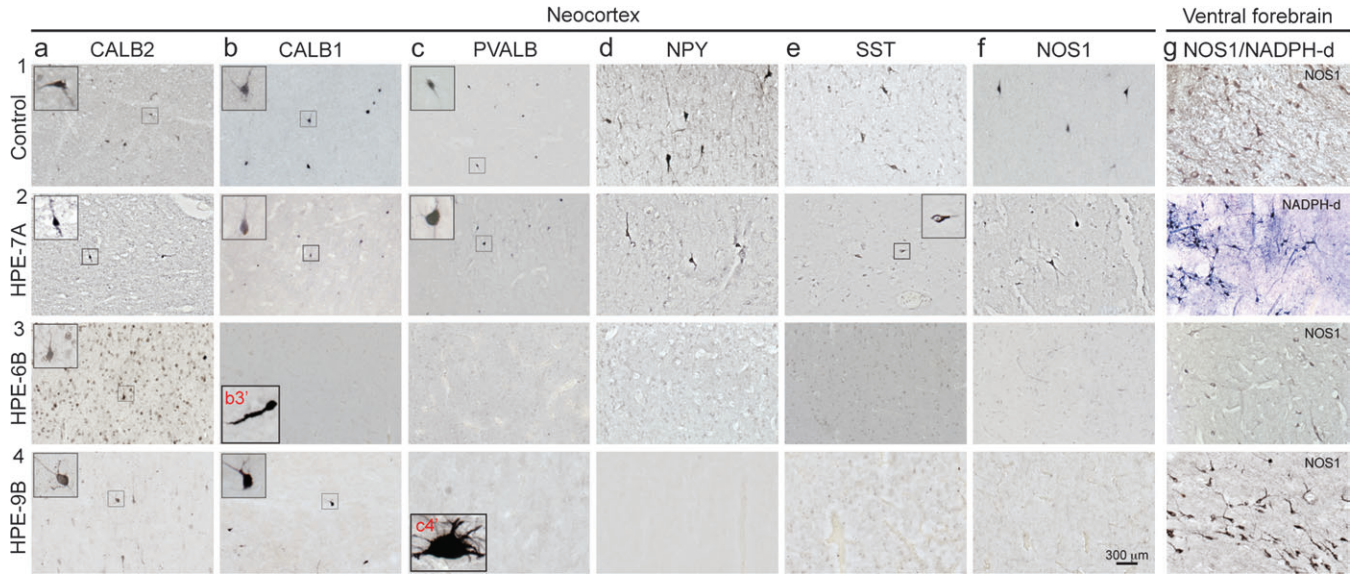

Figure 4. Representative images of immunohistochemistry for different interneuron markers at the border between the neocortical layer 6 and SP zone of age-matched control brains (1), an infant group A brain with moderately developed ventral forebrain (2; HPE-7A), and group B late fetal (3; HPE-6B) and early infant (4; HPE-9B) HPE brains with severe ventral forebrain hypoplasia. (*a1–4*) CALB2-positive interneurons are abundant in the neocortex of all cases. (*b1,2*) CALB1-positive interneurons are readily detected in control brains and the group A HPE brain. (*b3*) In group B late fetal HPE brain, CALB1-positive interneurons are not found in the neocortex but occasionally in the MZ/layer 1 and white matter (inset *b3'*). (*b4*) In group B infant HPE brain, CALB1-positive interneurons are found in markedly reduced numbers in the neocortex. (*c3,4–f3,4*) Cortical interneurons immunopositive for PVALB, NPY, SST, or NOS1 are almost completely absent from both late fetal and infant group B HPE brains but not from HPE-A cases or age-matched controls. (*c4*) occasional and morphologically aberrant PVALB-positive neurons were observed in the white matter of HPE-9B brain (inset *c4'*). (*g1–4*) NOS1/NADPH-d-positive interneurons could be detected in both late fetal and infant HPE striatum (*g1,2*) or rudimentary striatothalamic eminence (*g3,4*).

Depletion of NOS1/NPY/SST-Positive Striatal Interneurons in Human HPE Brains with Severe Striatal Hypoplasia

The depletion of NOS1/NPY/SST-positive interneurons in the cortex of HPE-B cases led us to question whether these interneurons are affected in the striatum of HPE cases. To examine this, we analyzed the expression for various interneuron markers in control and HPE tissue sections containing ventral forebrain structures. Numerous NOS1/NPY/SST- and CALB2-positive interneurons were found in the striatum starting from the early fetal stages in control brains (Supplementary Table 4; data not shown) (Sajin et al. 1992; Judas et al. 1999; Ulfig 2002; Meyer 2007). The same striatal interneurons were also readily found in all HPE-A cases (Supplementary Table 4). However, the number of NOS1/NPY/SST-positive, but not CALB2-positive, interneurons was dramatically reduced in the striatothalamic eminence of HPE-B brains (Figs. 3*c5,d5* and 4*g3,4* and data not shown), suggesting that their generation and differentiation were severely affected by the ventral forebrain maldevelopment in these brains. Interestingly, in some HPE-B brains (HPE-4B, -8B, and -9B), a small number of NOS1/NADPH-d/NPY/SST-positive interneurons were present in neuronal heterotopias near the corticostriatal border, the boundary between the developing neocortex and the ventral forebrain (Fig. 3*c4,d4*; data not shown). This observation suggests that migration defects of the remaining interneurons may also contribute to their absence from the cortex. Importantly, NOS1/NADPH-d/NPY/SST-positive neurons were present in the brain stem of all HPE-B brains in numbers comparable to control and HPE-A brains (Fig. 3*a6–d6*). Therefore, their absence in HPE-B cortex is not due to experimental failure or genomic disruption of these genes. Rather, their absence most likely represents a loss of these interneurons in the cortex and striatum as a consequence of defects in the development of ventral forebrain midline progenitor cells consistent with the severe striatal hypoplasia in HPE-B brains.

Depletion of TITF1-Positive Progenitors and Postmitotic Cells in the Ventral Forebrain of Human HPE Brains with Severe Striatal Hypoplasia

In rodents, cortical interneurons originate from molecularly distinct progenitor cells in the ganglionic eminences of the ventral forebrain (Wonders and Anderson 2006; Fishell 2007). These progenitors can be distinguished by the combinatorial expression of several transcription factors. Mouse *Dlx1/2* and *Ascl1* (also known as *Mash1*) are expressed throughout the proliferative zones of the ventral forebrain, and their loss in mice leads to severe reductions in the numbers of all major interneuron cell types (Anderson et al. 1997; Xu et al. 2004; Kim et al. 2008). To determine whether the subtype-specific absence of cortical interneurons in HPE-B cases is associated with alterations in distinct populations of interneuron progenitor cells, we analyzed expression of these transcription factors in control and HPE brains during the midfetal period using immunohistochemistry. We found DLX1/2- and ASCL1-positive cells throughout the proliferative zones of the ventral forebrain and cortical wall of all control and HPE brains (Figs. 5*a* and 6*a*,c; and Supplementary Table 4). Consistent with previous reports in the midfetal human brain (Letinic et al. 2002), we also observed that many of ASCL1-positive cells in proliferative zones of the ventral forebrain and neocortical wall coexpress Ki67, a marker of mitotic progenitor cells (50.2% and 27.0%, respectively) (Fig. 6*c*). Together, these findings

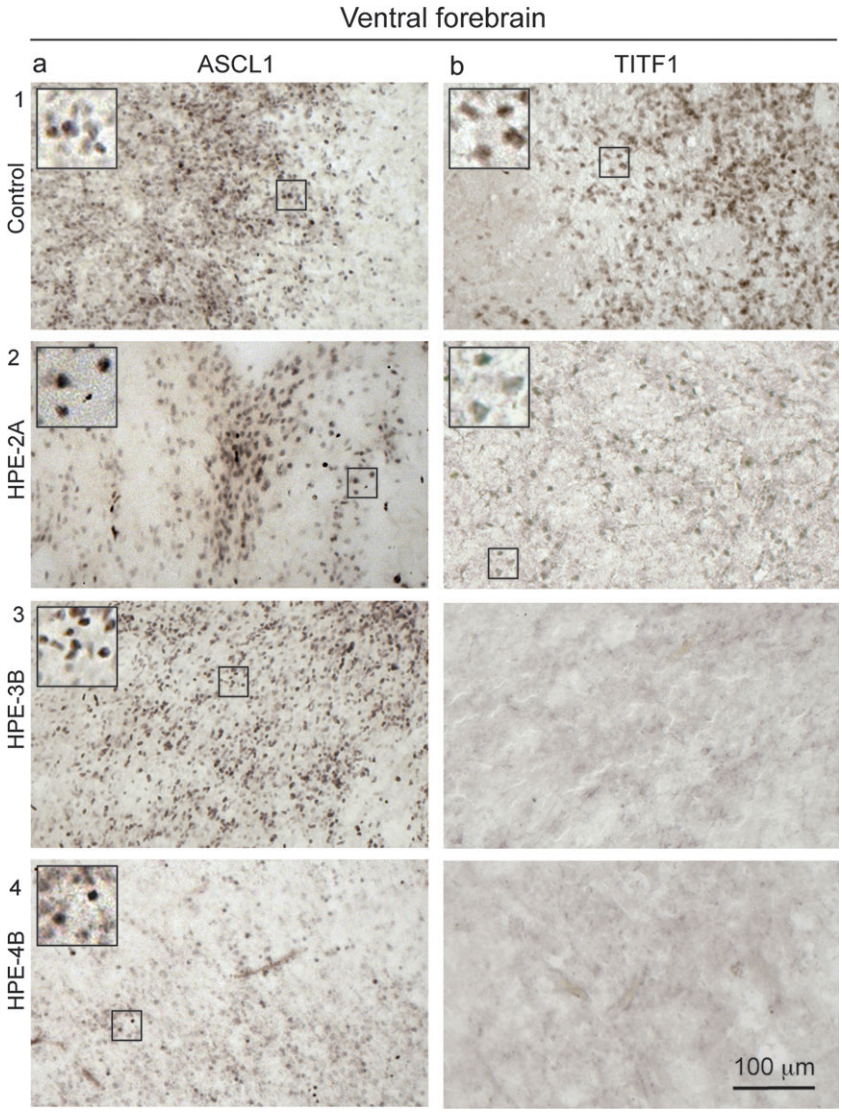

Figure 5. Representative images of immunohistochemical staining for different markers of putative progenitor cells of cortical interneurons in midfetal control and HPE-2A, -3B, and -4B brains. (*a1–4*) ASCL1, a pan-interneuronal progenitor cell marker, was immunodetected in the ventral forebrain ganglionic eminences and neocortical SVZ of all midfetal control and HPE A and B brains. (*b1–3*) Cells expressing *TITF1*, a marker of MGE progenitors, are present in control and HPE-2A striatum, but not in the rudimentary striatothalamic eminence of HPE-3B and 4B. Insets show enlarged views of the indicated area.

strongly suggest that the subtype-specific absence of interneurons in HPE-B cases is not associated with dramatic reduction of DLX1/2- and ASCL1-positive progenitor cells.

In contrast to *Dlx1/2* and *Ascl1*, mouse progenitor cells expressing *Titf1* (also known as *Nkx2.1*) are restricted to the medial ganglionic eminence (MGE) and give rise to both striatal and cortical NOS1/NPY/SST-positive interneurons (Xu et al. 2004; Wonders and Anderson 2006). Interestingly, in both control and HPE-A midfetal brains, we observed that cells expressing high levels of nuclear *TITF1* are mainly restricted to the ventral forebrain and, to a lesser extent, the corticostriatal border (Fig 5*b1,2* and Fig. 6*b*). Also consistent with previous data from mouse, 51.9% of TITF1-positive cells coexpressed Ki67 within the proliferative zones of the ventral forebrain at 18 and 20 wg (Fig. 6*c*), indicating that they are progenitor cells. Strikingly, TITF1-positive cells are dramatically depleted from the striatothalamic eminence and corticostriatal border of all HPE-B midfetal brains (Fig. 5*b3,b4*), indicating that the absence of TITF1-positive putative progenitors in the ventral forebrain is associated with the absence of NOS1/NPY/SST-positive cortical neurons in the same brains. Taken together, these findings indicate that human TITF1-positive neuronal progenitors are restricted to the ventral forebrain and dramatically depleted in HPE-B midfetal brains. Furthermore, consistent with previous studies in mice (Wonders and Anderson 2006), our results strongly indicate that human *TITF1* is downregulated in migrating and postmigratory cortical interneuron but maintained, at least during fetal and infantile periods, in many striatal interneurons. Finally, our findings suggest that a subtype of cortical interneurons expressing *NOS1*, *NPY*, and *SST*, and their putative ventral forebrain TITF1-positive MGE progenitors, are selectively more dramatically affected in human HPE with severe ventral forebrain hypoplasia.

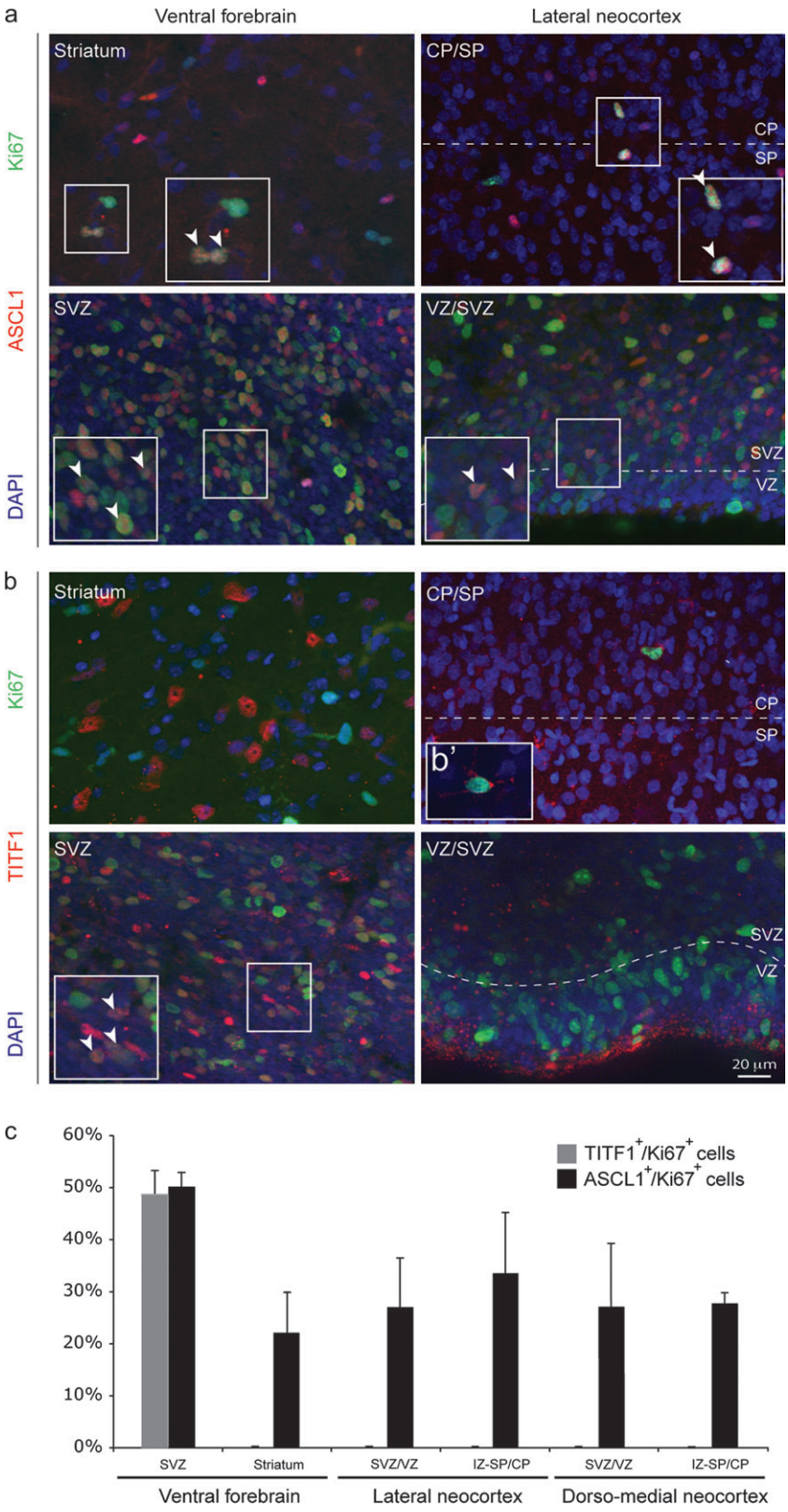

Figure 6. Analysis of proliferative TITF1- and ASCL1-positive cells in the dorsal and ventral forebrain of normal midfetal brains. (*a*,*b*) Both ASCL1- and TITF1-positive cells proliferate in the SVZ of ventral forebrain, as determined by the coexpression of Ki67, a mitotic cell marker (white arrowheads). (*a*–*c*) However, only nuclear stained ASCL1-positive cells colocalize with Ki67 within the striatum and throughout the dorsal VZ/SVZ, intermediate zone (IZ), and CP/SP border of the lateral and dorsal–medial neocortex. (*b'*), Cytoplasmic TITF1-positive cells were observed within the IZ and CP/SP in the midfetal neocortical wall. However, the specificity of this cytoplasmic immunolabeling, using anti-TITF1 antibody from Santa Cruz Biotechnology, has been questioned (Pan et al. 2004). Thus, cells with cytoplasmic immunostaining were not considered for the analysis. (*c*) The percentage of nuclear stained TITF1/Ki67-positive and ASCL1/Ki67-positive cells was estimated in both ventral and dorsal (lateral and dorso-medial neocortex) forebrain of Ctrl-1 (18 wg) and Ctrl-2 (20 wg) brains.

Cajal–Retzius, Subplate, and Cortical Projection Neurons are Present in HPE Brains with Severe Striatal Hypoplasia

To determine whether the migration and differentiation of other neuronal cell types are affected in human HPE, we analyzed neocortical and hippocampal cytoarchitecture using staining for Nissl substance and several well-characterized molecular markers of different subpopulations of CP and SP projection neurons. The basic cortical organization is relatively preserved in all HPE brains, as revealed by Nissl staining analysis (Supplementary Fig. 1). Importantly, the earliest generated reelin (RELN)-positive Cajal–Retzius neurons are clearly present in the MZ/layer 1 of all HPE brains (Fig. 7). RELN-positive Cajal–Retzius arise from distinct sources within the forebrain, including the dorsal midline (cortical hem) and the corticostriatal border, and are necessary for the proper "inside-out" neuronal migration and connectivity of cortical neurons (Soriano and Del Río 2005). Furthermore, our analysis of several markers of SP and CP layer-specific projection neurons [BCL11B (CTIP2), CUTL1 (CUX1), FEZF2 (FEZL, ZNF312), FOXP2, POU3F2 (BRN2), POU3F3 (BRN1), SMI-32, TBR1] (McEvilly et al. 2002; Ferland et al. 2003; Chen et al. 2005; Hevner 2007; Molyneaux et al. 2007; Kwan et al. 2008; Leone et al. 2008) revealed that these are expressed at the appropriate locations in both HPE group A and B neocortex (Fig. 8 and Supplementary Table 4). These findings suggest that the overall specification of cortical projection neurons is not dramatically affected in the analyzed HPE brains. Thus, our findings are consistent with previous studies of HPE animal models, which showed that defects in ventral or dorsal midline development do not severely affect the specification of cortical progenitors and projection neurons (Cheng et al. 2006; Rash and Grove 2007; Fernandes and Hébert 2008).

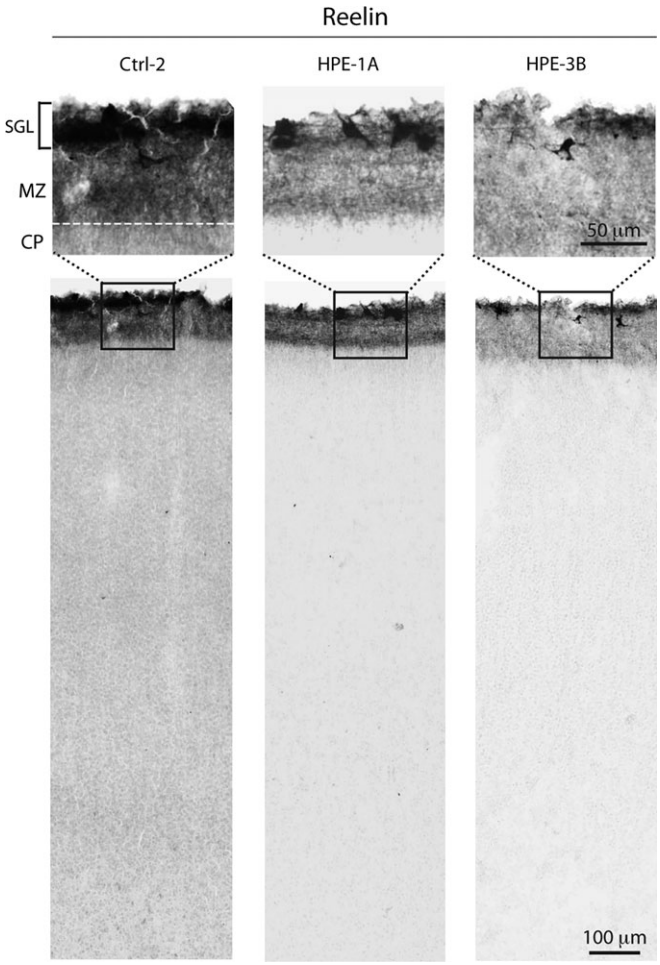

Figure 7. Reelin-positive Cajal–Retzius cells are present in the neocortex of midfetal HPE and age-matched control (Ctrl) brains. Subpial granular layer (SGL) and large Cajal–Retzius neurons in the MZ, the prospective layer 1, are labeled by anti-reelin antibody, in both HPE-1A and HPE-3B.

Discussion

In the present study, we show that human cortical interneurons, molecularly defined by the expression of *NOS1*, *NPY*, and *SST*, are either absent or dramatically reduced in the cortex of fetal and infant cases of HPE with severe ventral forebrain (striatal) hypoplasia (HPE-B). Furthermore, we provide evidence that PVALB-positive cortical interneurons, which normally are detected around the time of birth in the human neocortex, might be depleted from late fetal and infant HPE-B brains. However, because PVALB-positive interneurons appear in the cortex after other analyzed subpopulations and only small number of late fetal and infant cases have been analyzed in this study, additional analyses are necessary to substantiate this observation. Nevertheless, these results from late fetal and infant cases are consistent with our findings on NOS1/NPY/SST- and CALB2-positive cortical interneurons in HPE-B cases, as *CALB1* is coexpressed by these 2 subtypes of interneurons, and PVALB-positive cortical interneurons arise from the MGE progenitors like NOS1/NPY/SST-positive interneurons. In contrast, CALB2-positive interneurons were present in appropriate locations and significant numbers in the neocortex and hippocampus of all HPE cases, whereas CALB1-positive cortical interneurons were present in late fetal and infant HPE cases, even though in apparently reduced numbers. In addition, we show that Cajal–Retzius neurons, SP neurons, and CP projection neurons are not as dramatically affected in these HPE cases. Thus, our results indicate that development of NOS1/NPY/SST-positive interneurons is consistently and dramatically affected in human HPE with severe striatal hypoplasia.

Several lines of evidence suggests that the subpopulations of cortical interneurons expressing *NOS1*(NADPH-d)/*NPY*/*SST* are most likely lost in the HPE-B cases. First, all 3 of these molecular markers are concomitantly absent from the cortex of HPE-B brains. Second, their expression in the few remaining interneurons of the hypoplastic ventral forebrain or at the corticostriatal border is observed. And third, their absence correlated consistently with ventral forebrain hypoplasia. It is possible, though less likely, that cortical interneurons are present in the HPE-B cortex, but have simultaneously lost NOS1, NPY, and SST expressions. A more likely scenario is that the ventral forebrain hypoplasia in these cases has led to decreased generation and disrupted cortical migration of this subpopulation of interneurons.

The consistent depletion of NOS1/NPY/SST-positive cortical interneurons in all fetal and infant HPE-B cases with severe striatal hypoplasia was concomitant with the dramatic reduction in ventral forebrain cells expressing *TITF1*, whose mouse homolog is expressed by MGE progenitors and MGE-derived NOS1/NPY/SST interneurons (Wonders and Anderson 2006; Fishell 2007). Furthermore, these defects are reminiscent

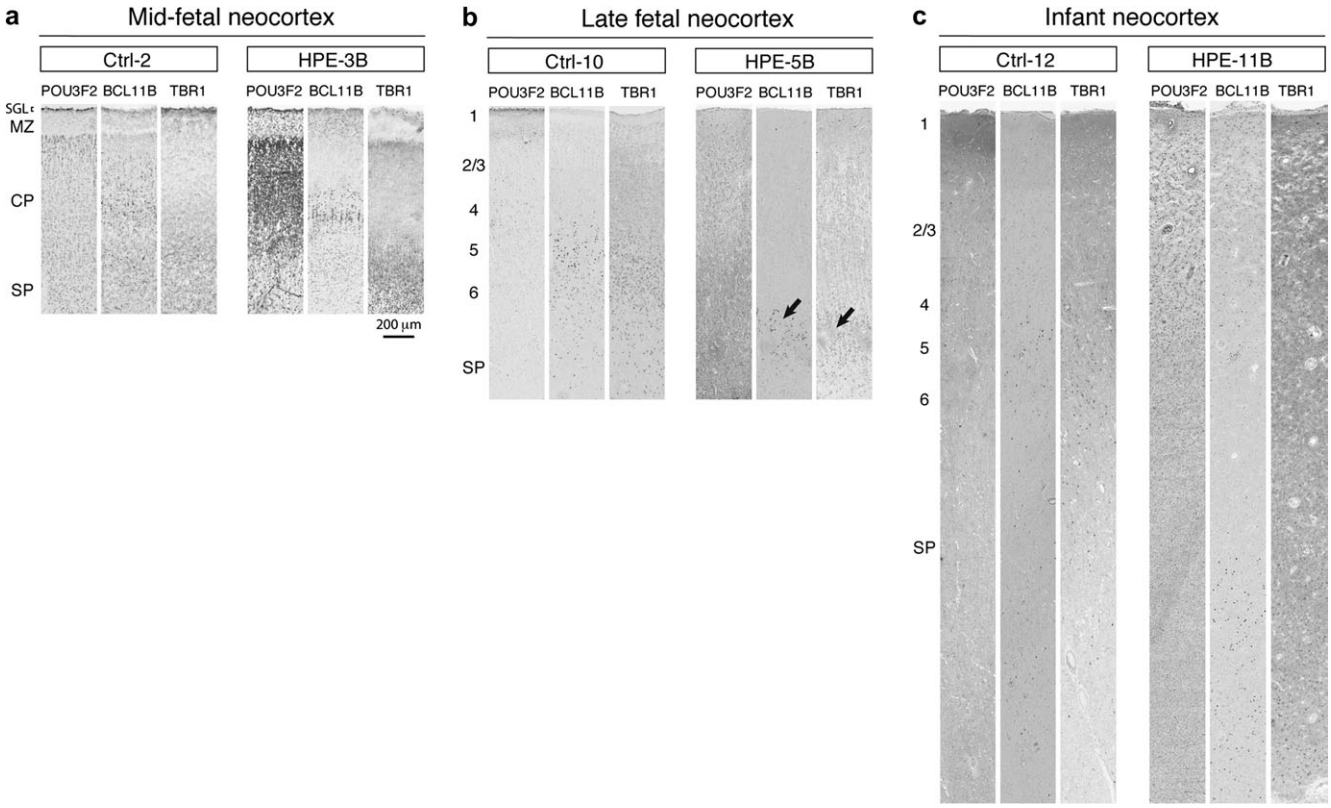

Figure 8. Immunohistochemical analysis of layer-enriched markers of neocortical projection neurons in midfetal, late fetal, and infant group B HPE brains and age-matched control (Ctrll) brains. Tissue sections of the midfetal (*a*), late fetal (*b*), and infant (*c*) frontal neocortex were immunostained with antibodies against TBR1 (layer 6 and 5), BCL11B (CTIP2) (layers 5 and 6), and POU3F2 (BRN2) (layers 2–5). Representative midfetal, late fetal, and infant HPE-B brains show a dense population of TBR1-positive neurons bordering the SP; large BCL11B-positive neurons positioned immediately above, and POU3F2-positive neurons scattered from layers 2 to 5, suggesting the correct sequence and development of the cortical layers. The black arrows point to coincident distribution of layers 5 and 6 projection neurons with glomerular structures formed by altered projection of axons and dendrites. SGL, subpial granular layer.

of those found in *Titf1*-deficient mice, which lack this subtype of striatal and cortical interneurons but not CALB2-positive cortical interneurons (Pleasure et al. 2000). Interestingly, the human *TITF1* homolog has been suggested as a candidate gene for HPE (Devriendt et al. 1998) and its haploinsufficiency causes benign hereditary chorea, a movement disorder associated with abnormal striatal interneurons (Breedveld et al. 2002). In contrast, cells expressing *DLX1/2* and *ASCL1*, markers of different interneuronal progenitor cells, were readily observed throughout the ventral and dorsal forebrain of all HPE and control midfetal cases, indicating that these putative interneuronal progenitors were less selectively affected in the same HPE cases. Interestingly, in mice, *Dlx1/2* and *Ascl1* are necessary for the development of *Calb2*-expressing cortical interneurons (Anderson et al. 1997; Xu et al. 2004), which in our HPE cases are not dramatically affected by severe ventral forebrain midline and striatal hypoplasia. Thus, our results show that NOS1/NPY/SST-positive cortical interneurons and related TITF1-positive progenitors are selectively and consistently more affected in HPE with ventral forebrain (striatal) hypoplasia. Furthermore, these findings are consistent with the possibility that at least a vast majority of NOS1/NPY/SST-positive interneurons are generated by TITF1-positive progenitors in the ventral forebrain and migrate dorsally into the cortex. Finally, this depletion of cortical inhibitory interneurons provides a possible pathophysiological mechanism for motor deficiencies and seizures often associated with HPE and characterize human HPE with severe ventral forebrain hypoplasia as a developmental "interneuronopathy" (Kato and Dobyns 2005).

The results of this study offer insights into the developmental origins of different cortical interneuron cell types. Consistent with previous findings (Judas et al. 1999; Ulfig 2002; Meyer 2007), we showed that molecularly defined cortical interneurons exhibit a distinct temporal sequence in their generation, migration routes, and differentiation during early human fetal development. For example, immature CALB2-positive interneurons with a migratory morphology were numerous in the lateral and caudal ganglionic eminences, paleocortical periventricular zone, and the subpial granular layer/MZ, and the subventricular zone (SVZ), the cortex (Meyer 2007; data not shown). In contrast, immature NOS1/NPY/SST-positive neocortical interneurons with a migratory morphology first appear around 15 wg in the neocortical SP and are scarce in the MZ or cortical SVZ (Judas et al. 1999; data not shown). These differences in the spatial distribution and molecular differentiation of these 2 main subtypes of human cortical interneurons are accompanied with differential distribution of markers associated with distinct subtypes of interneuronal progenitors. As previously described in the midfetal human and cynomolgus monkey, numerous ASCL1-positive putative progenitor cells and CALB2-positive interneurons are present in the dorsal pallial (cortical) proliferative zones (Letinic et al. 2002; Zecevic et al. 2005; Petanjek et al. 2008). Interestingly, our analysis revealed that ASCL1-positive cells were present in all HPE brains including those

lacking cortical NOS1/NPY/SST interneurons. This finding is consistent with the possibility that at least a portion of human cortical interneurons expressing *CALB2* is derived from neocortical ASCL1 (MASH1)-positive progenitors as previously described (Letinic et al. 2002). However, whether these ASCL1-positive progenitors, which in mice are known to give rise to both neuronal and glial cells (Kim et al. 2008), give rise to interneurons in human within the cortical proliferative zones during midfetal ages remains to be determined. Importantly, the correlation between the selective absence of a particular subtype of cortical interneurons and the disruption of TITF1-positive MGE progenitors in human HPE with severe ventral forebrain hypoplasia, together with the spatial and temporal differences in localization and differentiation of molecularly defined cortical interneurons in normal human fetal brain, suggests that different interneuron subtypes are derived from distinct progenitors.

Our results also provide insights into how different interneuron cell types may become more abundant during the development of the human cortex. Humans and other primates have a higher proportion of neocortical GABAergic neurons compared with rodent species (Gabbott and Bacon 1996; DeFelipe et al. 2006). Several studies indicate that this higher proportion of GABAergic interneurons is accompanied with an increase in molecular and morphological diversity and complexity of cell types (Lewis and Lund 1990; Hof et al. 2000; Preuss and Coleman 2002; DeFelipe et al. 2006). Though not specific to primates, *CALB2*-expressing double bouquet interneurons and tyrosine hydroxylase–expressing interneurons are especially abundant in the human neocortex, where they are thought to modulate the activity of a large variety of circuits (DeFelipe et al. 2006; Benavides-Piccione and DeFelipe 2007). Our findings are consistent with the possibility that developmental increases in cell number and spatial extension of specific interneuron progenitor pools, such as ASCL1-positive cells, have led to the selective amplification and dispersion of CALB2-positive, and perhaps other, interneurons in the developing human cerebral cortex.

Taken together, our findings indicate that the diversity of human cortical interneurons is established early during neurogenesis, with distinct subpopulations originating from spatially, temporally, and molecularly segregated pools of progenitors. Furthermore, our results are consistent with the possibility that the dorsal expansion of cortical CALB2-positive interneurons and the associated ASCL1-positive progenitor pool might contribute to the increased diversity of cortical interneurons and the formation of more elaborate cortical circuits in humans.

Supplementary Material

Supplementary material can be found at: http://www.cercor.oxfordjournals.org/

Funding

NIH (NS054273, HD045481) to N.S.; Portuguese Foundation for Science and Technology to S.F.; Autism Speaks to M-R.R.; Canadian Institutes of Health Research to K.Y.K; Croatian Ministry of Science, Education & Sport (108-1081870-1878) to M.J.

Notes

We thank J. Johnson for providing anti-ASCL1 antibodies; J. Arellano for stereological advice; B. Poulos for help with tissue acquisition; and M.B. Johnson, M. Mizuguchi, and P. Rakic for discussion and comments.

Conflict of Interest: None declared.

Address correspondence to Nenad Sestan, Department of Neurobiology, Yale University School of Medicine, PO Box 208001, New Haven, CT 06520-8001, USA. Email: nenad.sestan@yale.edu.

References

Anderson SA, Eisenstat DD, Shi L, Rubenstein JL. 1997. Interneuron migration from basal forebrain to neocortex: dependence on Dlx genes. Science. 278:474–476.

Arii N, Mizuguchi M, Mori K, Takashima S. 2000. Ectopic expression of telencephalin in brains with holoprosencephaly. Acta Neuropathol. 100:506–512.

Barkovich AJ, Quint DJ. 1993. Middle interhemispheric fusion: an unusual variant of holoprosencephaly. AJNR Am J Neuroradiol. 14:431–440.

Benavides-Piccione R, DeFelipe J. 2007. Distribution of neurons expressing tyrosine hydroxylase in the human cerebral cortex. J Anat. 211:212–222.

Breedveld GJ, van Dongen JW, Danesino C, Guala A, Percy AK, Dure LS, Harper P, Lazarou LP, van der Linde H, Joosse M, et al. 2002. Mutations in TITF-1 are associated with benign hereditary chorea. Hum Mol Genet. 11:971–979.

Chen JG, Rasin MR, Kwan KY, Sestan N. 2005. Zfp312 is required for subcortical axonal projections and dendritic morphology of deep-layer pyramidal neurons of the cerebral cortex. Proc Natl Acad Sci USA. 102:17792–17797.

Cheng X, Hsu CM, Currle DS, Hu JS, Barkovich AJ, Monuki ES. 2006. Central roles of the roof plate in telencephalic development and holoprosencephaly. J Neurosci. 26:7640–7649.

DeFelipe J, Ballesteros-Yáñez I, Inda MC, Muñoz A. 2006. Double-bouquet cells in the monkey and human cerebral cortex with special reference to areas 17 and 18. Prog Brain Res. 154:15–32.

DeMyer W. 1977. Holoprosencephaly. In: Vinken PJ, Bruyn GW, editors. Handbook of clinical neurology. Vol. 30. Amsterdam: Elsevier. p. 431–478.

Devriendt K, Fryns JP, Chen CP. 1998. Holoprosencephaly in deletions of proximal chromosome 14q. J Med Genet. 35:612.

Ferland RJ, Cherry TJ, Preware PO, Morrisey EE, Walsh CA. 2003. Characterization of Foxp2 and Foxp1 mRNA and protein in the developing and mature brain. J Comp Neurol. 460:266–279.

Fernandes M, Hébert JM. 2008. The ups and downs of holoprosencephaly: dorsal versus ventral patterning forces. Clin Genet. 73:413–423.

Fishell G. 2007. Perspectives on the developmental origins of cortical interneuron diversity. Novartis Found Symp. 288:21–35.

Gabbott PL, Bacon SJ. 1996. Local circuit neurons in the medial prefrontal cortex (areas 24a,b,c, 25 and 32) in the monkey: II. Quantitative areal and laminar distributions. J Comp Neurol. 364:609–636.

Golden JA. 1999. Towards a greater understanding of the pathogenesis of holoprosencephaly. Brain Dev. 21:513–521.

Hayashi M, Araki S, Kumada S, Itoh M, Morimatsu Y, Matsuyama H. 2004. Neuropathological evaluation of the diencephalon, basal ganglia and upper brainstem in alobar holoprosencephaly. Acta Neuropathol. 107:190–196.

Lewis DA, Lund JS. 1990. Heterogeneity of chandelier neurons in monkey neocortex: corticotropin-releasing factor- and parvalbumin-immunoreactive populations. J Comp Neurol. 293:599–615.

Hof PR, Glezer II, Nimchinsky EA, Erwin JM. 2000. Neurochemical and cellular specializations in the mammalian neocortex reflect phylogenetic relationships: evidence from primates, cetaceans, and artiodactyls. Brain Behav Evol. 55:300–310.

Hevner RF. 2007. Layer-specific markers as probes for neuron type identity in human neocortex and malformations of cortical development. J Neuropathol Exp Neurol. 66:101–109.

Jones EG. 1993. GABAergic neurons and their role in cortical plasticity in primates. Cereb Cortex. 3:361–372.

Judas M, Rasin MR, Kruslin B, Kostovic K, Jukic D, Petanjek Z, Kostovic I. 2003. Dendritic overgrowth and alterations in laminar phenotypes of neocortical neurons in the newborn with semilobar holoprosencephaly. Brain Dev. 25:32–39.

Judas M, Sestan N, Kostovic I. 1999. Nitrinergic neurons in the developing and adult human telencephalon: transient and

permanent patterns of expression in comparison to other mammals. Microsc Res Tech. 45:401–419.
Kato M, Dobyns WB. 2005. X-linked lissencephaly with abnormal genitalia as a tangential migration disorder causing intractable epilepsy: proposal for a new term, "interneuronopathy.". J Child Neurol. 20: 392–397.
Kawaguchi Y, Kondo S. 2002. Parvalbumin, somatostatin and cholecystokinin as chemical markers for specific GABAergic interneuron types in the rat frontal cortex. J Neurocytol. 31:277–287.
Kim EJ, Battiste J, Nakagawa Y, Johnson JE. 2008. Ascl1 (Mash1) lineage cells contribute to discrete cell populations in CNS architecture. Mol Cell Neurosci. 38:595–606.
Kubota Y, Hattori R, Yui Y. 1994. Three distinct subpopulations of GABAergic neurons in rat frontal agranular cortex. Brain Res. 649: 159–173.
Kwan KY, Lam MM, Krsnik Z, Kawasawa YI, Lefebvre V, Sestan N. 2008. SOX5 postmitotically regulates migration, postmigratory differentiation, and projections of subplate and deep-layer neocortical neurons. Proc Natl Acad Sci USA. 105:16021–16026.
Leone DP, Srinivasan K, Chen B, Alcamo E, McConnell SK. 2008. The determination of projection neuron identity in the developing cerebral cortex. Curr Opin Neurobiol. 18:28–35.
Letinic K, Zoncu R, Rakic P. 2002. Origin of GABAergic neurons in the human neocortex. Nature. 417:645–649.
Markram H, Toledo-Rodriguez M, Wang Y, Gupta A, Silberberg G, Wu C. 2004. Interneurons of the neocortical inhibitory system. Nat Rev Neurosci. 5:793–807.
McEvilly RJ, de Diaz MO, Schonemann MD, Hooshmand F, Rosenfeld MG. 2002. Transcriptional regulation of cortical neuron migration by POU domain factors. Science. 295:1528–1532.
Métin C, Baudoin JP, Rakić S, Parnavelas JG. 2006. Cell and molecular mechanisms involved in the migration of cortical interneurons. Eur J Neurosci. 23:894–900.
Meyer G. 2007. Genetic control of neuronal migrations in human cortical development. Adv Anat Embryol Cell Biol. 189:1–111.
Mizuguchi M, Morimatsu Y. 1989. Histopathological study of alobar holoprosencephaly. 1. Abnormal laminar architecture of the telencephalic cortex. Acta Neuropathol. 78:176–182.
Molyneaux BJ, Arlotta P, Menezes JR, Macklis JD. 2007. Neuronal subtype specification in the cerebral cortex. Nat Rev Neurosci. 8:427–437.
Monuki ES. 2007. The morphogen signaling network in forebrain development and holoprosencephaly. J Neuropathol Exp Neurol. 66:566–575.
Muenke M, Beachy PA. 2000. Genetics of ventral forebrain development and holoprosencephaly. Curr Opin Genet Dev. 10: 262–269.
Pan CC, Chen PC, Tsay SH, Chiang H. 2004. Cytoplasmic immunoreactivity for thyroid transcription factor-1 in hepatocellular carcinoma: a comparative immunohistochemical analysis of four commercial antibodies using a tissue array technique. Am J Clin Pathol. 21:343–349.
Petanjek Z, Berger B, Esclapez M. 2008. Origins of cortical GABAergic neurons in the cynomolgus monkey. Cereb Cortex. May 13 Epub access ahead of print.
Petilla Interneuron Nomenclature GroupAscoli GA, Alonso-Nanclares L, Anderson SA, Barrionuevo G, Benavides-Piccione R, Burkhalter A, Buzsáki G, Cauli B, Defelipe J, et al. 2008. Petilla terminology: nomenclature of features of GABAergic interneurons of the cerebral cortex. Nat Rev Neurosci. 9:557–568.
Pleasure SJ, Anderson S, Hevner R, Bagri A, Marin O, Lowenstein DH, Rubenstein JL. 2000. Cell migration from the ganglionic eminences is required for the development of hippocampal GABAergic interneurons. Neuron. 28:727–740.
Preuss TM, Coleman GQ. 2002. Human-specific organization of primary visual cortex: alternating compartments of dense Cat-301 and calbindin immunoreactivity in layer 4A. Cereb Cortex. 12:671–691.
Probst FP. 1979. The prosencephalies: morphology, neuroradiological appearances and differential diagnosis. Berlin (Germany): Springer-Verlag, Berlin.
Rash BG, Grove EA. 2007. Patterning the dorsal telencephalon: a role for sonic hedgehog? J Neurosci. 27:11595–11603.
Sajin B, Sestan N, Dmitrovic B. 1992. Compartmentalization of NADPH-diaphorase staining in the developing human striatum. Neurosci Lett. 140:117–120.
Sestan N, Kostovic I. 1994. Histochemical localization of nitric oxide synthase in the CNS. Trends Neurosci. 17:105–106.
Soriano E, Del Río JA. 2005. The cells of cajal-retzius: still a mystery one century after. Neuron. 46:389–394.
Takahashi TS, Kinsman S, Makris N, Grant E, Haselgrove C, McInerney S, Kennedy DN, Takahashi TA, Fredrickson K, Mori S, et al. 2004. Holoprosencephaly–topologic variations in a liveborn series: a general model based upon MRI analysis. J Neurocytol. 33:23–35.
Ulfig N. 2002. Calcium-binding proteins in the human developing brain. Adv Anat Embryol Cell Biol. 165:1–92.
Wonders CP, Anderson SA. 2006. The origin and specification of cortical interneurons. Nat Rev Neurosci. 7:687–696.
Xu Q, Cobos I, De La Cruz E, Rubenstein JL, Anderson SA. 2004. Origins of cortical interneuron subtypes. J Neurosci. 24:2612–2622.
Yakovlev PI. 1959. Pathoarchitectonic studies of cerebral malformations. III. Arhinencephalies(holotelencephalies). J Neuropathol Exp Neurol. 18:22–55.
Zecevic N, Chen Y, Filipovic R. 2005. Contributions of cortical subventricular zone to the development of the human cerebral cortex. J Comp Neurol. 491:109–122.

Supplementary Data:

Selective Depletion of Molecularly Defined Cortical Interneurons in Human Holoprosencephaly with Severe Striatal Hypoplasia

Sofia Fertuzinhos, Željka Krsnik, Yuka Imamura Kawasawa, Mladen-Roko Rašin, Kenneth Y. Kwan, Jie-Guang Chen, Miloš Judaš, Masaharu Hayashi & Nenad Šestan

SUPPLEMENTARY FIGURES LEGENDS

Supplementary Figure 1. Analysis of neocortical cytoarchitecture in Ctrl and HPE-A and –B cases by Nissl staining. Progressive thickening and lamination of the neocortex at the level of the frontal lobe in control brains. (*a*), Mid-fetal neocortex is composed of three compartments: the cortical plate (CP) and overlying marginal zone (MZ), forerunners of the mature cortical layers 1-6, and the subplate (SP). The MZ is characterized by a low cell density. The subpial granular layer (SGL) is present above the MZ. The CP appears as an intensely stained structure composed of densely packed, elongated neuronal cell bodies forming radial columns. The SP is composed of less densely packed cell bodies of heterogeneous size, shape, and orientation. The border between SP and CP can be clearly delineated. (*b*), Late fetal neocortex is characterized by the immature six-layered Grundtypen cortex of Brodmann with prominent future layer 4 in the middle. (*c*), During infancy the neocortex exhibits a more mature six-layered laminar pattern with sharp borders between individual layers and progressive differentiation of the large pyramidal neurons in layer 5 (*a*-*c*), Nissl staining reveals a preservation of the basic neocortical organization and lamination pattern in brains with HPE. All main compartments of the neocortical wall (SGL, MZ, CP, SP, white matter, and periventricular proliferative zones) are present in HPE brains. The neocortices of brains with HPE are thicker than those of age-matched controls. Stratification of the dysplastic neocortex into distinct layers is present, but varies considerably among cases and regions. Glomerular structures (arrows) formed by altered axons and dendrites are present within the neocortex of some HPE cases.

Supplementary Table 1. Description of control human brains analyzed in this study. Note that over 50 control brains not included in this table, ranging in age from 12 wg to newborn as well as different postnatal ages, were analyzed for NADPH-diaphorase staining, NOS1 immunohistochemistry, and some of the cell-type specific markers listed in Supplementary Table 3 (data not shown). AECOM, Albert Einstein College of Medicine Human Fetal Tissue Repository; BG, Basal ganglia; CIBR, Croatian Institute for Brain Research; Cryo, Cryopreserved; FFPE, Formalin fixed paraffin embedded; NA, Not available; ND, Not determined; OB, Olfactory bulb; PFA, Paraformaldehyde; TMIN, Tokyo Metropolitan Institute for Neuroscience; wg, weeks of gestation.

Supplementary Table 2. Description of human HPE brains analyzed in this study. HPE cases are organized by: 1) developmental stage, from earlier to later stages; 2) state of ventral forebrain/striatal development, from well-differentiated (group A) to hypoplastic (group B); and 3) age, from the youngest to oldest individual. AECOM, Albert Einstein College of Medicine Human Fetal Tissue Repository; CIBR, Croatian Institute for Brain Research; Cryo, Cryopreserved; FFPE, Formalin fixed paraffin embedded; NA, Not available; ND, Not determined; OB, Olfactory bulb; PFA, Paraformaldehyde; Str, striatum; TMIN, Tokyo Metropolitan Institute for Neuroscience; wg, weeks of gestation.

Supplementary Table 3. Description of all antibodies and *in situ* hybridization probes used in this study.

Supplementary Table 4. Summary of all histochemical, immunohistochemical staining and in situ hybridizations performed in all HPE cases and age-matched control brains. HPE cases are organized by: 1) developmental stage, from earlier to later stages; 2) ventral telencephalon hypoplasia severity, from less severe (group A) to more severe (group B); and 3) age, from the youngest to the oldest individual. The classifications are based on at least two independent experiments in different age-matched controls. The results were consistent from experiment to experiment. The degree of immunoreactivity is estimated within four levels: - indicates absence of positive cells; -/+ corresponds

to occasional positive cells; + corresponds to a low number of positive cells; ++ corresponds to a moderate number of positive cells; and +++ corresponds to a high number of positive cells. (a) Immunostaining for SMI32, a marker of differentiating layer 3 and 5 pyramidal neurons, appeared earlier in the mid-fetal HPE brains than in age-matched controls. (b) The first SST-positive interneurons appear around 21 to 22 wg in the control neocortex and striatum. (c) A small number of CALB1+, resembling Cajal-Retzius neurons, were present in the marginal zone of the hippocampus of mid-fetal control and HPE brains. (d) Even though PVALB-positive cortical interneurons should be present in the neocortex from 26-32 wg, in our control brains we can only observe PVALB-positive cortical interneurons in infant control brains. Of all HPE-B brains only HPE-9B and -10B cases exhibited very scarse and morphologically aberrant PVALB-positive cells in the white matter. (e) Occasional TITF1+ cells were detected in the mid-fetal white matter, subventricular zone, and lower subplate. This expression pattern is consistent with the down regulation of mouse *Titf1* expression in MGE-derived NOS1/NPY-positive interneurons migrating to the cortex (data not shown). (f) Occasional NADPH-d-reactive and NOS1/NPY-positive cells were detected in the striato-thalamic eminences of HPE-3B. (g) DLX1/2 immunostaining appears to be diminished in mid-fetal HPE cases in comparison to age-matched controls. However, no specific immunostaining pattern could be found in paraffin-embedded tissue sections from late fetal and infant HPE cases or age-matched controls. (h) Tissue sections containing the rudimentary striato-thalamic eminence of HPE-4B brains were used for other analyses. (i) The subpial granular layer normally disappears during the late fetal period and is not present in infancy. (j) NADPH-d histochemistry and SMI-32 immunostaining were performed on cryopreserved tissue sections of HPE-7A. These stainings did not work on tissue sections from paraffin-embedded blocks. (k) GABA immunohistochemistry did not produce a specific staining pattern on HPE-9B tissue, likely because of prolonged tissue fixation. Inc (Inconclusive), immunostaining with certain antibodies and NADPH-d histochemistry did not yield specific staining patterns using paraffin-embedded control or HPE tissue. NA, the striatum and brain stem from HPE-4 were not available for this study. NT, not tested.

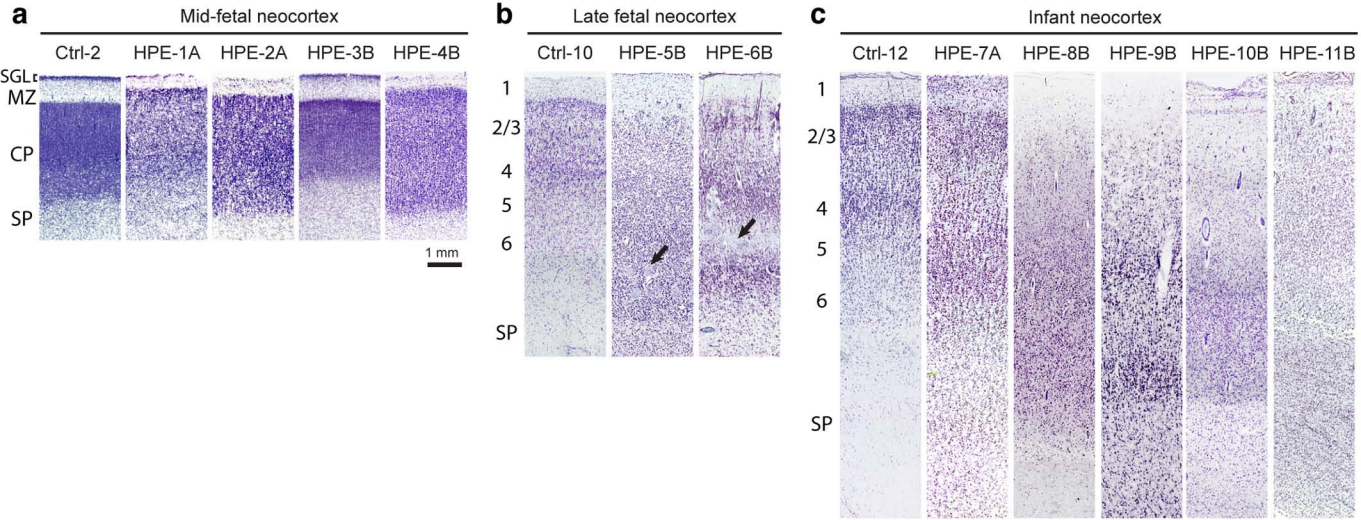
a
Mid-fetal neocortex
Ctrl-2
HPE-1A
HPE-2A
HPE-3B
HPE-4B
SGLE
MZ
CP
SP
1 mm
b
Late fetal neocortex
Ctrl-10
HPE-5B
HPE-6B
1
2/3
4
5
6
SP
c
Infant neocortex
Ctrl-12
HPE-7A
HPE-8B
HPE-9B
HPE-10B
HPE-11B
1
2/3
4
5
6
SP

Case	Age	Gender	Post-mortem delay (hours)	Facial abnormalities	Gross brain abnormalities	Genetic abnormalities	Maternal ethinicity	Maternal age (years)	Maternal medical history	Cigarette, drug, alcohol abuse	Source	Histological notes
Ctrl-1	18 wg	F	≤ 1hr	None	None	ND	Hispanic	28	Healthy	NA	AECOM	PFA and Cryo
Ctrl-2	20 wg	F	≤ 1hr	None	None	ND	Hispanic	19	Healthy	NA	AECOM	PFA and Cryo
Ctrl-3	20 wg	M	≤ 1hr	None	None	ND	NA	16	Sickle cell trait (asymptomatic); UTI (Rx); anemia (no Rx)	NA	AECOM	PFA and Cryo
Ctrl-4	20 wg	M	≤ 1hr	None	None	ND	Caucasian	20	Healthy	None	AECOM	PFA and Cryo. Serially sectioned forebrain.
Ctrl-5	21 wg	M	≤ 1hr	None	None	ND	Hispanic	ND	NA	NA	AECOM	PFA and Cryo
Ctrl-6	22 wg	F	≤ 1hr	None	None	ND	African American	ND	Healthy	NA	AECOM	PFA and Cryo. Serially sectioned forebrain.
Ctrl-7	22 wg	M	≤ 1hr	None	None	ND	NA	15	Elevated white blood cells	None	AECOM	PFA and Cryo
Ctrl-8	24 wg	F	≤ 1hr	None	None	ND	African American		Asthma (no Rx)	NA	AECOM	PFA and Cryo
Ctrl-9	24 wg	F	≤ 1hr	None	None	ND	African American	26	abNI PAP	None	AECOM	PFA and Cryo
Ctrl-10	30 wg	M	3 hr	None	None	ND	Asian	20s	Healthy	None	TMIN	FFPE
Ctrl-11	37 wg	M	2 hr	None	None	ND	Asian	20s	Healthy	None	TMIN	FFPE
Ctrl-12	3 months	F	6 hr	None	None	ND	Caucasian	NA	NA	NA	CIBR	PFA; Cryo and FFPE
Ctrl-13	4 months	F	3 hr	None	None	ND	Asian	20s	Healthy	None	TMIN	FFPE
Ctrl-14	12 months	M	3 hr	None	None	ND	Asian	20s	Healthy	None	TMIN	FFPE

	Case	Group	Age	Gender	Post-mortem delay (hours)	Facial abnormalities	Dorsal forebrain	Ventral forebrain	Genetic abnormalities	Maternal ethinicity	Maternal age (years)	Maternal medical history	Cigarette, drug, alcohol abuse	Source	Histological notes
Mid-fetal	HPE-1	A	20 wg	F	≤1 hr	Cleft lip and palate	Partial medial longitudinal fissure	Moderately developed Str. Present OB.	ND	African American	16	Healthy	None	AECOM	PFA and Cryo
	HPE-2	A	24 wg	F	≤1 hr	Cleft lip and palate	Partial medial longitudinal fissure	Well-developed Str. Present OB.	FISH results uninterpretable	NA	35	NA	None	AECOM	PFA and Cryo
	HPE-3	B	20 wg	NA	≤1 hr	Cleft lip and palate	No medial longitudinal fissure	Severely hypoplastic Str. Absent OB.	ND	Hispanic	23	Healthy	None	AECOM	PFA and Cryo
	HPE-4	B	24 wg	F	≤1 hr	Cleft lip and palate	No medial longitudinal fissure	Severely hypoplastic Str. Absent OB.	Trisomy of chromosome 18 or 13	Hispanic	24	Healthy	20 cigarettes/day	AECOM	PFA and Cryo
Late fetal	HPE-5	B	31 wg	F	3 hr	Ethmocephaly	No medial longitudinal fissure	Severely hypoplastic Str.	ND	Asian	NA	Pregnancy complications due to toxemia.	None	TMIN	FFPE
	HPE-6	B	35 wg	F	3 hr	Ethmocephaly	No medial longitudinal fissure	Severely hypoplastic Str.	ND	Asian	NA	NA	None	TMIN	FFPE
Infant	HPE-7	A	4 months	F	≤2 hr	Cleft lip and palate	Partial medial longitudinal fissure.	Moderately developed Str. Present OB.	ND	Caucasian	NA	NA	NA	CIBR	FFPE or Cryo
	HPE-8	B	1 month	F	3 hr	Cleft lip and palate	No medial longitudinal fissure	Severely hypoplastic Str.	ND	Asian	NA	NA	None	TMIN	FFPE
	HPE-9	B	2 months	F	ND	Cleft lip and palate	Partial occipital lobes	Severely hypoplastic Str.	ND	Caucasian	NA	NA	NA	CIBR	PFA and Cryo
	HPE-10	B	7 months	F	8 hr	Cleft lip and palate	No medial longitudinal fissure	Severely hypoplastic Str.	ND	Asian	29	Healthy	None	TMIN	FFPE
	HPE-11	B	12 months	F	2 hr	Cleft lip and palate	No medial longitudinal fissure	Severely hypoplastic Str.	ND	Asian	27	Pregnancy complications due to increased sugar in urine, unrelated to diabetes.	None	TMIN	FFPE

Neuronal cell-type specific markers	Description	Reagent source and information
Subpial granular zone interneurons		
Calbindin 2, 29kDa (Calretinin) (CALB2)	Calcium-binding protein enriched in migrating interneurons	Swant /6B3/ Mouse/1:2000; Swant/7699-4/Rabbit/1:100
Cajal-Retzius (CR) neurons		
Reelin (RELN)	Protein secreted by CR neurons in the marginal zone	CR50 antibody/Mouse/1:100; Chemicon/MAB5364/Mouse/1:500; Santa Cruz/ sc-32556/Goat/1:100
Calbindin 2, 29kDa (Calretinin) (CALB2)	Calcium-binding protein colocalizes with reelin positive neurons in the marginal zone	Swant /6B3/ Mouse/1:2000; Swant/7699-4/Rabbit/1:100
T-box brain gene 1 (TBR1)	Transcription factor colocalizes with RELN^{+} neurons	Chemicon/AB9616/Rabbit/1:100
SMI-32	Non-phosphorylated epitopes in Neurofilament H (NEFH)	Sternberger Monoclonals/SMI32 antibody/Mouse/1:1000; Covence/SMI-32R/Mouse/1:500
Cortical plate projection neurons		
Forkhead box P2 (FOXP2)	Transcription factor expressed by layer 6 and 5 neurons	Sestan lab/Rabbit/1:500; Novus Biologicals /ab1307/Rabbit/1:750
T-box brain gene 1 (TBR1)	Transcription factor enriched in layer 6 and 5 neurons	Chemicon/AB9616/Rabbit/1:100
B-cell CLL/lymphoma 11B (BCL11B; CTIP2)	Transcription factor expressed by layer 6 and 5 neurons	Abcam/ab18465/Rat/1:500
FEZ family zinc finger 2 (FEZF2; FEZL; ZNF312)	Transcription factor expressed by layer 6 and 5 neurons	Sestan lab/Rabbit/1:100; in situ hybridization
SMI-32	Non-phosphorylated epitopes in Neurofilament H (NEFH); enriched in layers 5 and 3	Sternberger Monoclonals/SMI32 antibody/Mouse/1:1000
POU domain, class 3, transcription factor 3 (POU3F3; BRN1)	Transcription factor enriched in layer 4 - 2 neurons	Santa Cruz Biot./sc-6028/Goat/1:100
POU domain, class 3, transcription factor 2 (POU3F2; BRN2)	Transcription factor enriched in layer 4 - 2 neurons	Santa Cruz Biot./sc-6029/Goat/1:100
Subplate projection neurons		
Forkhead box P2 (FOXP2)	Expressed by putative projection neurons	Sestan lab/Rabbit/1:500; Novus Biologicals/ab1307/Rabbit/1:750
T-box brain gene 1 (TBR1)	Expressed by putative projection neurons	Chemicon/AB9616/Rabbit/1:100
FEZ family zinc finger 2 (FEZF2; FEZL; ZNF312)	Expressed by putative projection neurons	Sestan lab/Rabbit/1:100; in situ hybridization
SMI-32	Enriched in putative projection neurons	Sternberger Monoclonals/SMI32 antibody/Mouse/1:1000
Cortical/Subplate interneurons		
GABA	Marker of all cortical interneurons	Sigma/A 2052/Rabbit/1:2000
Nitric oxide synthase 1, neuronal (NOS1; nNOS)	Highly enriched in NPY/SST interneurons	Zymed/61-7000/Rabbit/1:500;ImmunoStar/24431 & 24287/Rabbit/1:2000
NADPH-diaphorase	Histochemical marker of nitric oxide synthase (NOS)	See Methods
Neuropeptide Y (NPY)	Neuropeptide in NOS1/NADPH-d/SST interneurons	Sigma/N 9528/Rabbit/1:100; Santa Cruz/sc-14728 /Goat/1:100
Somatostatin (SST)	Neuropeptide in NOS1/NADPH-d/SST interneurons	Peninsula Laboratories/T-4103/Rabbit/1:100; Chemicon/AB5494/Rabbit/1:1000
Calbindin 2, 29kDa (Calretinin; CALB2)	Calcium-binding protein	Swant /6B3/ Mouse/ 1:2000; Swant/7699-4/Rabbit/1:100
Calbindin 1, 28kDa (CALB1)	Calcium-binding protein	Swant/300/Mouse/1:1000; Sigma/C 9848/Mouse/1:100
Parvalbumin (PVALB)	Calcium-binding protein	Swant/235/Mouse/1:5000
Thyroid transcription factor 1 (TITF1; NKX2.1)	Transcription factor expressed by migrating MGE-derived interneurons	Santa Cruz Biotech/sc-8761/Goat/1:150; Biopat/Rabbit/1:150
Cortical SVZ interneuronal progenitors		
Aschaete-scute complex homolog 1 (ASCL1; MASH1)	Transcription factor expressed by SVZ progenitors	Gift from Jane Johnson/Mouse-Ascl1/1:2; Rabbit-Ascl1/1:500
Striatal projection neurons		
B-cell CLL/lymphoma 11B (BCL11B; CTIP2)	Expressed by the majority of striatal projection neurons	Abcam/ab18465/Rat/1:500
POU domain, class 3, transcription factor 3 (POU3F3; BRN1)	Expressed by the majority of striatal projection neurons	Santa Cruz Biotechnology/sc-6028/ Goat/ 1:100
POU domain, class 3, transcription factor 2 (POU3F2; BRN2)	Expressed by many striatal projection neurons	Santa Cruz Biotechnology/sc-6029/ Goat/ 1:100
Striatal interneurons		
GABA	Marker of non-cholinergic striatal interneurons	Sigma/A 2052/Rabbit/1:2000
Nitric oxide synthase 1, neuronal (NOS1; nNOS)	Highly enriched in NPY/SST interneurons	Zymed/61-7000/Rabbit/1:500;ImmunoStar/24431 & 24287/Rabbit/1:2000
NADPH-diaphorase	Histochemical marker of nitric oxide synthase (NOS)	See Methods
Neuropeptide Y (NPY)	Neuropeptide in NOS1/NADPH-d/SST interneurons	Sigma/N 9528/Rabbit/1:100; Santa Cruz/sc-14728 /Goat/1:100
Somatostatin (SST)	Neuropeptide in NOS1/NADPH-d/SST interneurons	Peninsula Laboratories/T-4103/Rabbit/1:100; Chemicon/AB5494/Rabbit/1:1000
Calbindin 2, 29kDa (Calretinin) (CALB2)	Calcium-binding protein	Swant /6B3/ Mouse/ 1:2000; Swant/7699-4/Rabbit/1:100
Calbindin 1, 28kDa (CALB1)	Calcium-binding protein	Swant/300/Mouse/1:1000; Sigma/C 9848/Mouse/1:100
Parvalbumin (PVALB)	Calcium-binding protein	Swant/235/Mouse/1:5000
Subpallium interneuronal progenitors		
Aschaete-scute complex homolog 1 (ASCL1; MASH1)	Transcription factor expressed by progenitors from LGE, MGE and CGE	Gift from Jane Johnson/Mouse-Ascl1/1:2; Rabbit-Ascl1/1:500
Distal-less homeobox 1 (DLX1)	Transcription factor expressed by subpalial SVZ interneuron progenitors	Chemicon/AB5724/Rabbit
Distal-less homeobox 2 (DLX2)	Transcription factor expressed by subpalial SVZ interneuron progenitors	Chemicon/AB5726/Rabbit/1:100;Abcam/ab18188/Rabbit/1:100;St Cruz/sc-18140/Goat/1:100
Thyroid transcription factor 1 (TITF1; NKX2.1)	Expressed by MGE progenitors and MGE-derived striatal interneurons	Santa Cruz Biotech/sc-8761/Goat/1:150; Biopat/Rabbit/1:150

Neuronal cell-type specific markers	Mid-fetal					Late fetal			Infant					
	Ctrl 1-9	HPE-1A	HPE-2A	HPE-3B	HPE-4B	Ctrl 10 and 11	HPE-5B	HPE-6B	Ctrl 12-14	HPE-7A	HPE-8B	HPE-9B	HPE-10B	HPE-11B
Subpial granular zone interneurons														
CALB2 (calretinin)	+++	+++	+++	+++	+++	-/+ *(i)*	-/+	-/+	- *(i)*	-	-	-	-	-
Cajal-Retzius neurons														
RELN	+++	+++	+++	+++	+++	*Inc*	*Inc*	*Inc*	*Inc*	NT	*Inc*	+	*Inc*	*Inc*
CALB2	+++	+++	+++	+++	+++	+++	+++	+++	+	+	+	+	++	++
TBR1	+++	++	+++	+++	++	+	+	+	-/+	NT	-/+	-/+	-/+	-/+
SMI-32	-/++	-/+	++	+++	+++	*Inc*	*Inc*	*Inc*	*Inc*	+ *(j)*	*Inc*	+ *(j)*	*Inc*	*Inc*
Cortical plate projection neurons														
FOXP2	+++	+++	+++	+	++	*Inc*	*Inc*	*Inc*	*Inc*	*Inc*	*Inc*	*Inc*	*Inc*	*Inc*
TBR1	+++	+++	+++	+++	+++	+++	+++	+++	++	NT	++	+	+++	++
BCL11B (CTIP2)	+++	+++	+++	+++	+++	*Inc*	*Inc*	*Inc*	*Inc*	*Inc*	*Inc*	*Inc*	*Inc*	*Inc*
FEZF2 (FEZL; ZNF312)	+++	NT	NT	+++	+++	NT	NT	NT	NT	NT	NT	NT	NT	NT
SMI-32	- *(a)*	++	+++	+++	+++	*Inc*	*Inc*	*Inc*	*Inc*	++ *(j)*	*Inc*	++ *(j)*	*Inc*	*Inc*
POU3F3 (BRN1)	+++	+++	+++	+++	+++	*Inc*	*Inc*	*Inc*	*Inc*	*Inc*	*Inc*	*Inc*	*Inc*	*Inc*
POU3F2 (BRN2)	+++	+++	+++	+++	+++	*Inc*	*Inc*	*Inc*	*Inc*	*Inc*	*Inc*	*Inc*	*Inc*	*Inc*
Subplate projection neurons														
FOXP2	++	++	++	+	++	*Inc*	*Inc*	*Inc*	*Inc*	*Inc*	*Inc*	*Inc*	*Inc*	*Inc*
TBR1	++	+++	+++	+++	+++	+++	+++	+++	+	NT	++	+	+++	+
FEZF2 (FEZL; ZNF312)	++	-	-	++	++	*Inc*	*Inc*	*Inc*	*Inc*	*Inc*	*Inc*	*Inc*	*Inc*	*Inc*
SMI-32	-/+ *(a)*	-/+	+	++	++	*Inc*	*Inc*	*Inc*	*Inc*	++ *(j)*	*Inc*	++ *(j)*	*Inc*	*Inc*
Cortical/Subplate interneurons														
GABA	+++	+++	+++	++	++	*Inc*	*Inc*	*Inc*	*Inc*	*Inc*	*Inc*	*Inc (k)*	*Inc*	*Inc*
NOS1 (nNOS)	+++	++	++	-	-	+++	-	-	+++	++	-	-	-	-
NADPH-diaphorase	+++	++	++	-	-	*Inc*	*Inc*	*Inc*	*Inc*	++ *(j)*	*Inc*	*Inc*	*Inc*	*Inc*
NPY	+++	++	++	-	-	+++	-	-	+++	++	-	-	-	-
SST	-/+ *(b)*	-	+	-	-	+++	-	-	+++	++	-	-	-	-
CALB2 (calretinin)	+++	+++	+++	+++	+++	+++	+++	+++	+++	+++	+++	+++	+++	+++
CALB1 (calbindin 1)	-/+ *(c)*	+ *(c)*	+ *(c)*	-/+ *(c)*	+ *(c)*	++	-/+	-	+++	+++	-	++	-/+	+
PVALB (parvalbumin)	- *(d)*	-	-	-	-	+ *(d)*	-	-	*Inc (d)*	++	-	-/+ *(d)*	-/+ *(d)*	-
TITF1 (NKX2.1)	+ *(e)*	+	+	-	-/+	*Inc*	*Inc*	*Inc*	*Inc*	*Inc*	*Inc*	NT	*Inc*	*Inc*
Cortical SVZ progenitors														
ASCL1 (MASH1)	++	+	++	++	+	+++	+	++	++	NT	-/+	++	++	++
Striatal projection neurons														
BCL11B (CTIP2)	+++	NA	+++	++	++	*Inc*	*Inc*	*Inc*	*Inc*	*Inc*	*Inc*	*Inc*	*Inc*	*Inc*
POU3F3 (BRN1)	+++	NA	+++	++	++	*Inc*	*Inc*	*Inc*	*Inc*	*Inc*	*Inc*	*Inc*	*Inc*	*Inc*
POU3F2 (BRN2)	++	NA	++	++	++	*Inc*	*Inc*	*Inc*	*Inc*	*Inc*	*Inc*	*Inc*	*Inc*	*Inc*
Striatal interneurons														
GABA	+++	NA	+++	++	++	*Inc*	*Inc*	*Inc*	*Inc*	*Inc*	*Inc*	*Inc (k)*	*Inc*	*Inc*
NOS1 (nNOS)	+++	NA	+++	-/+ *(f)*	+	+++	+++	+++	++	NT	++	+++	+++	++
NADPH-diaphorase	+++	NA	+++	-/+ *(f)*	+	+++	*Inc*	*Inc*	*Inc*	++	*Inc*	*Inc*	*Inc*	*Inc*
NPY	+++	NA	+++	-/+ *(f)*	NT *(h)*	+++	+	+	+++	NT	+	ND	+	+
SST	-/+ *(b)*	NA	+	-	NT *(h)*	++	++	++	+++	NT	++	++	++	++
CALB2 (calretinin)	+++	NA	+++	++	++	++	++	++	+++	NT	+++	+++	+++	++
CALB1 (calbindin 1)	-/+	NA	-/+	+	NT *(h)*	++	+	++	+++	NT	++	+++	+++	+++
PVALB (parvalbumin)	-	NA	-	-	NT *(h)*	+	+	+	++	NT	-	++	++	+
Subpallium interneuronal progenitors														
ASCL1 (MASH1)	+++	NA	+++	++	+	+++	++	++	+++	NT	-/+	+++	++	++
DLX1	+++ *(g)*	NA	+	+	+	*Inc*	*Inc*	*Inc*	*Inc*	*Inc*	*Inc*	*Inc*	*Inc*	*Inc*
DLX2	+++ *(g)*	NA	+	+	+	*Inc*	*Inc*	*Inc*	*Inc*	*Inc*	*Inc*	*Inc*	*Inc*	*Inc*
TITF1 (NKX2.1)	+++	NA	++	-	NT *(h)*	*Inc*	*Inc*	*Inc*	*Inc*	*Inc*	*Inc*	NT	*Inc*	*Inc*